Tran-SET

Transportation Consortium of South-Central States

*Solving Emerging Transportation Resiliency, Sustainability, and Economic Challenges through the Use of Innovative Materials and Construction Methods: From Research to Implementation*

# Determination of the Optimal Parameters for Self-Healing Efficiency of Encapsulated Bacteria in Concrete Simulated Subtropical Climate

**Project No. 20CLSU05**

**Lead University: Louisiana State University**

**Final Report**

**March 2022**

**Disclaimer**

The contents of this report reflect the views of the authors, who are responsible for the facts and the accuracy of the information presented herein. This document is disseminated in the interest of information exchange. The report is funded, partially or entirely, by a grant from the U.S. Department of Transportation's University Transportation Centers Program. However, the U.S. Government assumes no liability for the contents or use thereof.

**Acknowledgements**

The authors would also like to acknowledge the laboratory support from the Louisiana Transportation Research Center, the technical expertise and feedback of Dr. Gary King. The authors would also like to acknowledge the work and contributions from Ricardo Hungria, Omar Omar, and Andrea Gavilanes.

# TECHNICAL DOCUMENTATION PAGE

| 1. Project No. | 2. Government Accession No. | 3. Recipient's Catalog No. |
|---|---|---|
| 20CLSU05 | | |

| 4. Title and Subtitle | 5. Report Date |
|---|---|
| Determination of the Optimal Parameters for Self-Healing Efficiency of Encapsulated bacteria in Concrete Simulated Subtropical Climate | August 2021 |
| | **6. Performing Organization Code** |
| **7. Author(s)** | **8. Performing Organization Report No.** |
| PI: Momen R. Mousa https://orcid.org/0000-0002-1723-364X<br>Co-PI: Marwa Hassan https://orcid.org/0000-0001-8087-8232<br>Co-PI: Gabriel A. Arce https://orcid.org/0000-0002-3610-8238<br>GRAs: Ricardo Hungria, Andrea Gavilanes, Omar Kamal | |
| **9. Performing Organization Name and Address** | **10. Work Unit No. (TRAIS)** |
| Transportation Consortium of South-Central States (Tran-SET)<br>University Transportation Center for Region 6<br>3319 Patrick F. Taylor Hall, Louisiana State University, Baton Rouge, LA 70803 | **11. Contract or Grant No.**<br>69A3551747106 |
| **12. Sponsoring Agency Name and Address** | **13. Type of Report and Period Covered** |
| United States of America<br>Department of Transportation<br>Research and Innovative Technology Administration | Final Research Report<br>Aug. 2020 – Jan. 2022 |
| | **14. Sponsoring Agency Code** |

**15. Supplementary Notes**

Report uploaded and accessible at Tran-SET's website (http://transet.lsu.edu/).


**16. Abstract**

Concrete is a remarkable construction material. However, its low tensile strength makes it prone to cracking, which negatively affects its durability. To address this issue, bacterial concrete has been implemented as a self-healing alternative due to its capability to seal microcracks through microbial-induced calcium carbonate precipitation (MICCP). In this study, a bacterial strain (i.e, Bacillus Pseudiformus) was encapsulated through three different methods: encapsulation through hydrogel beads, vacuum impregnation on lightweight aggregates, and attachment to cellulose nanocrystals. Furthermore, three precursor types were used, magnesium acetate, calcium lactate, and sodium lactate were implemented. Compressive strength tests and flexural strength tests were performed on mortar specimens to characterize their mechanical properties. Once the crack was induced, samples were subjected to 28 days of wet/dry cycles in which the corresponding crack width was monitored. At the end of this period, the beams were retested to determine the strength recovery of the specimens. The results showed that the specimen groups in which calcium lactate was added to the cementitious matrix displayed the highest values in compressive strength. In terms of flexural strength, no major difference was found among the specimens. Moreover, the flexural strength recovery of the specimens did not show any significant difference as well. In terms of the healing efficiency, the sample that displayed the best results was the one containing calcium lactate as a precursor along with bacteria and yeast extract encapsulated in hydrogel beads. In addition, scanning electron microscopy (SEM) along with x-ray energy dispersive spectroscopy (EDS) was performed on the cracked specimens to characterize the healing products. Furthermore, a scale study was performed on concrete samples to determine the long-term implications of adding encapsulated bacteria along with calcium lactate and yeast extract in concrete.


| 17. Key Words | 18. Distribution Statement |
|---|---|
| Self-healing concrete, bacteria, MICP, microbial induced calcite precipitation, spores, bio concrete, healing agent, biomineralization | No restrictions. This document is available through the National Technical Information Service, Springfield, VA 22161. |

| 19. Security Classif. (of this report) | 20. Security Classif. (of this page) | 21. No. of Pages | 22. Price |
|---|---|---|---|
| Unclassified | Unclassified | 43 | |

**Form DOT F 1700.7 (8-72)** **Reproduction of completed page authorized.**

# SI* (MODERN METRIC) CONVERSION FACTORS

## APPROXIMATE CONVERSIONS TO SI UNITS

| Symbol | When You Know | Multiply By | To Find | Symbol |
|---|---|---|---|---|
| | | **LENGTH** | | |
| in | inches | 25.4 | millimeters | mm |
| ft | feet | 0.305 | meters | m |
| yd | yards | 0.914 | meters | m |
| mi | miles | 1.61 | kilometers | km |
| | | **AREA** | | |
| $in^2$ | square inches | 645.2 | square millimeters | $mm^2$ |
| $ft^2$ | square feet | 0.093 | square meters | $m^2$ |
| $yd^2$ | square yard | 0.836 | square meters | $m^2$ |
| ac | acres | 0.405 | hectares | ha |
| $mi^2$ | square miles | 2.59 | square kilometers | $km^2$ |
| | | **VOLUME** | | |
| fl oz | fluid ounces | 29.57 | milliliters | mL |
| gal | gallons | 3.785 | liters | L |
| $ft^3$ | cubic feet | 0.028 | cubic meters | $m^3$ |
| $yd^3$ | cubic yards | 0.765 | cubic meters | $m^3$ |
| | | NOTE: volumes greater than 1000 L shall be shown in $m^3$ | | |
| | | **MASS** | | |
| oz | ounces | 28.35 | grams | g |
| lb | pounds | 0.454 | kilograms | kg |
| T | short tons (2000 lb) | 0.907 | megagrams (or "metric ton") | Mg (or "t") |
| | | **TEMPERATURE (exact degrees)** | | |
| $^oF$ | Fahrenheit | 5 (F-32)/9<br>or (F-32)/1.8 | Celsius | $^oC$ |
| | | **ILLUMINATION** | | |
| fc | foot-candles | 10.76 | lux | lx |
| fl | foot-Lamberts | 3.426 | candela/$m^2$ | $cd/m^2$ |
| | | **FORCE and PRESSURE or STRESS** | | |
| lbf | poundforce | 4.45 | newtons | N |
| $lbf/in^2$ | poundforce per square inch | 6.89 | kilopascals | kPa |

## APPROXIMATE CONVERSIONS FROM SI UNITS

| Symbol | When You Know | Multiply By | To Find | Symbol |
|---|---|---|---|---|
| | | **LENGTH** | | |
| mm | millimeters | 0.039 | inches | in |
| m | meters | 3.28 | feet | ft |
| m | meters | 1.09 | yards | yd |
| km | kilometers | 0.621 | miles | mi |
| | | **AREA** | | |
| $mm^2$ | square millimeters | 0.0016 | square inches | $in^2$ |
| $m^2$ | square meters | 10.764 | square feet | $ft^2$ |
| $m^2$ | square meters | 1.195 | square yards | $yd^2$ |
| ha | hectares | 2.47 | acres | ac |
| $km^2$ | square kilometers | 0.386 | square miles | $mi^2$ |
| | | **VOLUME** | | |
| mL | milliliters | 0.034 | fluid ounces | fl oz |
| L | liters | 0.264 | gallons | gal |
| $m^3$ | cubic meters | 35.314 | cubic feet | $ft^3$ |
| $m^3$ | cubic meters | 1.307 | cubic yards | $yd^3$ |
| | | **MASS** | | |
| g | grams | 0.035 | ounces | oz |
| kg | kilograms | 2.202 | pounds | lb |
| Mg (or "t") | megagrams (or "metric ton") | 1.103 | short tons (2000 lb) | T |
| | | **TEMPERATURE (exact degrees)** | | |
| $^oC$ | Celsius | 1.8C+32 | Fahrenheit | $^oF$ |
| | | **ILLUMINATION** | | |
| lx | lux | 0.0929 | foot-candles | fc |
| $cd/m^2$ | candela/$m^2$ | 0.2919 | foot-Lamberts | fl |
| | | **FORCE and PRESSURE or STRESS** | | |
| N | newtons | 0.225 | poundforce | lbf |
| kPa | kilopascals | 0.145 | poundforce per square inch | $lbf/in^2$ |

# TABLE OF CONTENTS

## LIST OF FIGURES

## LIST OF TABLES

## ACRONYMS, ABBREVIATIONS, AND SYMBOLS

| | |
|---|---|
| ASTM | American Society for Testing and Materials |
| CH | Calcium Hydroxide |
| CNC | Cellulose Nanocrystals |
| CSH | Calcium Silicate Hydrate |
| EDS | Energy Dispersive Spectroscopy |
| HSD | Honest Significant Difference |
| LWA | Lightweight aggregate |
| LTRC | Louisiana Transportation Research Center |
| MICP | Microbial Induced Calcite Precipitation |
| mM/l | Millimolar/liter |
| SEM | Scanning Electron Microscope |
| RH | Relative Humidity |

# EXECUTIVE SUMMARY

Concrete is one of the most popular construction materials globally due to its remarkable attributes such as cost-effectiveness, high compressive strength, and easiness of work. Nevertheless, its weakness when subjected to tension makes it prone to cracking. Cracking increases permeability, creating a pathway for oxygen, moisture, carbon dioxide, and chloride ions to penetrate the structure, jeopardizing durability.

Bacterial concrete has become one of the most promising autogenous healing alternatives due to its capability to seal cracks with a width up to 1 mm. This remarkable feature occurs through a phenomenon known as microbial-induced calcite precipitation (MICP), where through bacterial activity, calcium carbonate is deposited in the cracks of the cementitious matrix, hence sealing them. The success of the MICP reaction depends on the presence of water, oxygen, mineral precursor, nutrients, bacteria, and a calcium source. Furthermore, wet/dry cycles have been identified as the ideal curing conditions to maximize the self-healing capacity of concrete. Moreover, the wet/dry cycles tend to simulate subtropical conditions characterized by intense periods of rain followed by dry periods, making this self-healing technology appropriate for this type of weather.

In this study, the authors implemented three different encapsulation procedures to protect the bacteria during the concrete mixing process. The three different methods correspond to encapsulation in hydrogel beads, vacuum impregnation on lightweight aggregates (LWA), and attachment of bacteria to cellulose nanocrystals. The bacteria strain implemented in each of these encapsulation methods corresponds to Bacillus pseudiformus. In addition, three different precursor types were investigated namely magnesium acetate, calcium lactate, and sodium lactate. The mechanical characterization of the specimens was performed through cubes for compressive strength tests and beams for flexural strength tests. Furthermore, after 28 days of wet/dry cycles, the beams were rested to determine the strength recovery. Moreover, during these wet/dry cycles, the cracked specimens were monitored to determine the respective healing efficiency. Finally, after the last flexural strength test, the specimens were salvaged and subjected to scanning electron microscopy (SEM) and x-ray energy dispersive spectroscopy (EDS) to characterize the healing products

The results from the mechanical tests indicated that the addition of calcium lactate as a precursor is beneficial in terms of compressive strength, disregarding the encapsulation method. Nevertheless, for the LWA impregnation method, the compressive strength results are lower compared to the rest of the specimens. This behavior is attributed to the porosity of the specimens, which negatively affects this mechanical property. Furthermore, the three-point bending tests revealed that most of the specimens did not display a substantial difference in terms of flexural strength. Moreover, once the specimens were retested under bending after the 28 days of wet/dry cycles, the results indicated there was not any substantial difference in flexural strength recovery among all the specimens.

In terms of the self-healing efficiency, the samples that displayed the best results were the ones in which calcium lactate along with bacteria and yeast extract were encapsulated into hydrogel beads, followed by specimens in which sodium lactate was impregnated along with bacteria and yeast extract. Moreover, even though it did not display the overall best results, the specimens containing calcium lactate long with bacteria attached with CNCs, displayed the best results for this particular encapsulation method. These results indicate that the best precursor among the implemented for

bacterial concrete purposes is calcium lactate. Furthermore, after the last flexural tests, all the samples were salvaged, and the cracked specimens were subjected to scanning electron microscopy (SEM) and x-ray energy dispersive spectroscopy (EDS) to characterize the healing products. The results from these analyses revealed on the specimen containing calcium lactate along with bacteria and yeast extract have a combination of calcium-rich crystals and calcium silicate hydrate (CSH) like products. These healing products are attributed to a combination of bacterial activities along with the further hydration of the cement process, which was enhanced by the action of the wet/dry cycles and the hydrogel beads which acted as a water reservoir.

After the analysis in mortar specimens was performed, a scale-up analysis was conducted in concrete samples to determine if the results obtained by the mortar specimens were obtained in concrete. As for the compressive and flexural strength, it was shown that the addition of calcium lactate was beneficial for the mechanical properties of the specimens. In terms of the self-healing efficiency results, the control specimens outperformed the specimens' containing bacteria and calcium lactate. However, their results were deemed promising since they outperformed previous works. The healing products characterization was also performed for these specimens, which indicated that calcite was the main product. Nevertheless, vaterite was shown in bacteria and calcium lactate-containing specimens, showing that there was still room for more healing, hence it was concluded that the investigation on the scale-up analysis shall be extended to see the long-term implications of this material.

The overall results indicated that bacteria encapsulated in hydrogel beads along with calcium lactate as precursor and yeast extract as a nutrient displayed the best results, for the self-healing of the mortar specimens. Nevertheless, a previous study on bacterial concrete has shown that vacuum impregnation on LWA containing calcium lactate as a precursor has developed promising and satisfactory results. Therefore, a last check and comparison with this encapsulation method shall be performed.

# 1. INTRODUCTION

Concrete is a widely used construction material because of its attributes such as cost-effectiveness, high compressive strength, and easiness of work (*1*). However, it has its limitation in withstanding high tensile stresses that make it prone to cracking. The crack formation can expose the steel reinforcement to environmental substances (i.e., oxygen, moisture, carbon dioxide, and chloride ions) that can penetrate the concrete and jeopardize its transport and mechanical properties. Thus, the use of self-healing technologies has been studied to address this challenge. Self-healing techniques, including the use of expansive mineral admixtures, self-control tight-crack width cementitious composites such as Engineered Cementitious Composites (ECC), chemicals in glass tubing or microcapsules, have been studied for concrete applications (*2*). Moreover, the addition of bacteria in concrete has also been studied as a self-healing technology mainly because of its capability to seal cracks with a width of less than 1 mm without human intervention(*3*, *4*). The healing process in bacterial concrete occurs as a result of a reaction known as microbial induced calcite precipitation (MICP). In the MICP process, the bacteria participate in the precipitation of calcium carbonate ($CaCO_3$) in the mortar matrix to seal cracks (*5*).

The success of MICP is determined by the presence of water, mineral precursors, bacteria, nutrients, and a calcium source (*6*, *7*). However, concrete provides a harsh environment for bacteria; therefore, it needs to be protected. This kind of environment is harmful because the pores in concrete close up to $0.5\mu m$ and the size of the bacteria is 1-3 $\mu m$ (*4*). Several protection techniques have been implemented from the use of hydrogel beads to vacuum impregnation into light weight aggregates (*8*, *9*). Furthermore, a novel technology that has been applied in concrete has been the addition of cellulose nanocrystals (CNCs). The incorporation of these crystals has been found beneficial for the mechanical properties of concrete (*10*). Knowing this, the present report also aims to be the pioneer in adding CNCs and bacteria for self-healing concrete purposes. The mineral precursor is another factor in the MICP process. Megalla studied the use of calcium lactate in mortar specimens, reaching a healing efficiency of up to 99% (*1*). In the work of Irwan et al., the addition of calcium lactate in bacterial concrete gave as a result an increase of 18.9% in the compressive strength (*11*). In the same study, the water penetration decreased up to 32.2% compared to the control mixture set. Magnesium acetate is another precursor that has been studied. Soysal et al. analyzed the addition of magnesium acetated and yeast extract for bacterial concrete, obtaining up to 68% of crack healing efficiency after 28 days of wet/dry cycles (*12*). In addition, sodium lactate and yeast extract have been used as broth for bacterial growth (*13*, *14*). However, its effects as a precursor in bioconcrete have not been evaluated.

As aforementioned, the presence of water and oxygen, have been found relevant for the MICP reaction. Therefore, wet/dry cycles have been vastly investigated in order to provide the proper conditions for self-healing concrete applications. The effect of wet/dry cycles has been studied by Wang et al.; for this purpose, multiple conditions were examined including complete water immersion, complete immersion in a deposition medium (DM), dry conditions at 20°C, 95% relative humidity (RH), wet/dry cycles with water and wet/dry cycles with DM. Each wet/dry cycle consisted of 16 hours of immersion, followed by 8 hours of dry conditions. Among the different conditions, the wet/dry cycles with water displayed the best results in terms of self-healing efficiency for bioconcrete purposes (*4*). Similarly, a study performed by Hassan et al. utilized wet/dry cycles in a relatively hot environment to simulate subtropical climate, which includes heavy rain periods follow by dry times. This study aims to determine which precursor

along with which impregnation method in subtropical climate conditions is better for bacterial concrete applications

## 2. OBJECTIVES

The main objective of this study was to determine which precursor and encapsulation method can optimize the self-healing efficiency of encapsulated bacteria in concrete in a subtropical climate. To achieve this objective, 21 sets of mortar specimens were prepared, three different precursor types were implemented, and three different encapsulation methods were studied. The three different methods were encapsulation into hydrogel beads, vacuum impregnation on lightweight aggregates (LWA), and attachment to cellulose nanocrystals (CNCs). All the specimens were subjected to compressive strength tests, flexural strength tests, crack width measurements, and scanning electron microscopy (SEM) along with energy dispersive x-ray spectroscopy (EDS). Once the best performing sample was determined, a scale-up study was conducted on concrete specimens. Moreover, these specimens were resubjected to the aforementioned tests in order to determine the effects of incorporating precursors along with bacteria in concrete

# 3. LITERATURE REVIEW

## 3.1 Metabolic Pathways

Depending on the type of bacteria, the MICP reaction can be triggered in different ways. Ideally, the bacteria type should be alkaliphiles meaning that they should be able to survive in an alkaline environment, with pH typically ranging between 8.5 to 11. In bacterial concrete applications, there are three pathways: urea hydrolysis, nitrogen reduction, and conversion of organic salts

### *3.1.1 Urea hydrolysis*

This metabolic pathway corresponds to the most commonly researched MICP process in bioconcrete applications. It consists of ureolytic bacteria strains (i.e., Bacillus megaterium, bacillus sphaericus, bacillus pasteuii), which once embedded in the concrete can heal it by biomineralization produced by bacteria urease enzyme activities in a calcium-rich environment (*15*). The rate of $CaCO_3$ precipitation is influenced by several factors: the availability of urea, which acts as the precursor, the availability of the nutrient (i.e., yeast extract), the presence of water along with calcium, and the bacteria´s urease activity.

This pathway occurs by the decomposition of urea and carbonate ions, where the carbonate reacts with the free calcium ions present in the cementitious matrix. It is possible to quantify the amount of bacterial activity by measuring the quantity of decomposed urea, based on the total ammonium nitrogen present in the system, considering that one mole of urea can produce two moles of ammonium. Nevertheless, it is essential to note that the production of ammonium can potentially be prejudicial to the concrete since it contributes to the leaching of calcium hydroxide, which is similar to what occurs during an acid attack (*16*, *17*).

### *3.1.2 Nitrogen Reduction*

The reduction of nitrates by biological means takes place when nitrate instead of oxygen, is utilized by the bacteria for respiring (*2*). In this pathway when an organic salt is dissolved during the denitrification process, the living organism produces $CO_2$ which in a solution generates carbonate ions. These carbonate ions later react with the free calcium ions present in the cementitious matrix yielding calcium carbonate. One advantage of this metabolic pathway is that it does not require oxygen for the bacteria to respire; so, it does not starve, which could be prejudicial to the entire system by reducing the calcite precipitation rate. Furthermore, this MICP reaction includes nitrite, which can inhibit corrosion in reinforced concrete with steel (*18*). It is relevant to note that the presence of water, nitrate, a calcium source, and a mineral precursor is essential for the success of this metabolic pathway.

Calcite precipitation through nitrogen reduction has been thoroughly researched for soil reinforcement with different bacteria strains, including Castellaniella Denitrificans (*19*), Pseudomonas Denitrificans (*20*), Diaphorobacter Nitroreducens and Pseudomanas Aureginosa (*18*) and Synechococcus PCC8806 (*21*). A peculiar bacteria strain corresponds to Synechococcus PCC8806, which corresponds to an auto-phototrophic cyanobacterium that generates $CaCO_3$ by photosynthesis and has the capability to heal concrete since it can live in high alkaline environments and to produce $CaCO_3$ that could withstand sonication of mortar cubes. Diaphorobacter Nitroreducens and Pseudomonas Aureginosa correspond to two bacteria species that were observed to generate high quantities of calcium carbonate and also were likely to survive in conditions where nutrient availability was limited (*22*).

Moreover, these bacteria strains were impregnated through a vacuum chamber in two aggregate types, expanded clays, and granular activated carbon particles. Once the aggregates were impregnated, they were mixed in the mortar mix. Mortar specimens were cast and tested under a uniaxial tension after 28 days of curing to induce cracking. Once the specimens were cracked, they were subjected to 28 days of water immersion to produce the crack healing through calcite precipitation. For the specimens containing Diaphorobacter Nitroreducens, after 14 days of water immersion, the cracks with a width of approximately 350 um were closed by more than 90%. After 28 days these cracks experienced complete healing. In the case of the specimens containing Pseudomonas Aeruginosa bacteria strain, until day 21 of immersion, the crack healing results did not substantially differ from the abiotic control. Nevertheless, at age 28 days, the healing efficiency results significantly outperformed the abiotic control.

In terms of the nutrients for these bacteria strains, calcium nitrate seems to be a promising option due to its excellent compatibility with cementitious materials (*2*). Calcium nitrate is frequently implemented as an admixture in concrete due to its ability to act like a set accelerator, corrosion inhibitor, and compressive strength enhancer. Other mineral precursors that have been used for these bacteria species are calcium lactate and calcium formate since they do not provoke any detrimental effects on the concrete (*18*).

### *3.1.3 Conversion of Organic Salts*

This pathway refers to the conversion of organic salts by bacterial respiration in order to generate $CO_2$ (*2*). In contact with water, carbon dioxide dissolves and produces carbonate ions. Within a calcium-rich environment, such as the cementitious matrix, the carbonate ions react with the calcium ions forming $CaCO_3$. Furthermore, the amount of precipitated calcium carbonate can be increased if the $CO_2$ generated by bacterial means reacts with the calcium hydroxide present in the concrete, forming more calcite crystals. There are several factors that determine the success of the MICP reaction for this particular pathway, including the availability of oxygen, the presence of water, a calcium source, and the type of organic salt or precursor.

The bacterial activities that take place during the MICP reaction for this pathway can be quantified by measuring the amount of oxygen consumed by the bacterial culture. Another factor essential for this pathway's success is the selection of the mineral precursor along with its concentration, which should not jeopardize the properties of the concrete. Several research works have found that nutrients such as yeast extract, calcium acetate, and peptone can be detrimental to the concrete's compressive strength (*23*). Nevertheless, a precursor type that has been shown to enhance the concrete properties is calcium lactate, which has been found to increase the compressive strength of concrete when directly added to the mix (*11*). In terms of self-healing efficiency, successful results have been reported when bacteria strains such as Bacillus pseudiformus, Bacillus Cohnii, and Bacillus alkalinitrilicus have been implemented (*7*, *23*).

### *3.1.4 Bacterial Strain Selection*

Considering the successful results the conversion of organic salts has obtained in the past, bacteria strains that utilized this metabolic pathway were chosen as possible candidates for this project(*7*). Regarding the bacteria selection, Sharma et al. (*24*) studied the effect of three different alkaliphilic Bacillus species on self-healing concrete. The bacteria were *Bacillus pseudofirmus*, *Bacillus cohnii* and *Bacillus halodurans*. In that work, spores of the bacteria were placed onto the concrete and the survival rate along with $CaCO_3$ precipitated were quantified. The authors found that after three days of curing, *Bacillus cohnii* had a survival rate of 0.25%; after days 7 and 28, the survival rate

decreased from 0.15% to 0.09%. For *Bacillus halodurans*, the survival rate after 3 and 7 days was 0.24% and 0.1%, respectively. The survival rate for *Bacillus pseudofirmus* bacteria was 1.4% after 3 days, and 1% after day 28. In addition, *Bacillus pseudofirmus* gave more amount of $CaCO_3$. In the study of Jonkers et al., *Bacillus pseudofirmus* with calcium lactate was compared to control mixture concrete sets. Control mixture sets displayed crystals precipitation of 1 to 5 $\mu m$ of size, while mixtures with *Bacillus pseudofirmus* showed mineral-like particles on the cracks with sized of 20-80 $\mu m$ (*23*). Due to these satisfactory results, *Bacillus pseudofirmus* was chosen as the bacteria strain for this study.

## 3.2 Encapsulation Procedures

### *3.2.1 Hydrogel Beads*

The hydrogel beads encapsulation method has been deemed by scientists to become a feasible method for inducing bacterial activity autonomously (*2*). Typically, hydrogel beads are manufactured from alginate; which is a natural polysaccharide obtained from algae (*25*). There are two approaches to generating alginate gels: ionic crosslinking (ionic gels) or acid precipitation (acidic gels). In the case of ionic cross-linking, the alginate gelation is done by the binding of divalent cations and a polymeric structure known as G-block. In a particular manner, the incorporation of calcium ions in the polymer binds the G chains. This alignment generates a diamond-shaped hole with a hydrophilic cavity, which unites the calcium ions by multi-coordination using the atoms of oxygen to create carboxyl groups. The generated polymers are so strongly bound, that they end up showing an egg-box shape. As for the alginic acid hydrogels, they are formed when the pH of the solution is lowered below disassociation constants ($pK_a$). The drop in pH affects the alginate solution in two particular ways. If the pH reduction happens at a high speed, the precipitation of alginate molecules will occur in the form of aggregates. If the reduction in the pH displays a steady drop, the result will display a continuous acid bulk gel. It is relevant to state that the acidic alginate gels happen to stabilize by hydrogen bonding followed by M blocks residues, which have displayed an important role in gelation.

As for the methods implemented for producing gel particles, the size of the gel plays a relevant factor. Two main categories are possible according to the gel size, macrogels, which occur when the gel particle diameter is beyond 1000 um, and microgels when the diameter is less than 1000 um. A last category is nanogels, which occur when the gel size is less than 500 nm. The macrogels are commonly produced through a process denominated simple dripping or extrusion. This method includes the extrusion of alginate droplets from a syringe, then the droplets fall into a gelling bath (*25*). Once the droplets reach the needle tip, they start growing until they are big enough to detach and get into the bath. The size of the macrogels produced on this method, commonly ranges between 1 to 2 mm (*26*).

Furthermore, the morphology and the size of the gel particle can change according to the viscosity of the alginate, the height between the alginate and the exit point, and the needle diameter (*27*). The particle sphericity is determined by the distance between the bath and the exit point. The gel droplet can lose its shape if the surface tension forces and the solution´s viscosity cannot overcome the surface tension of the gelling bath (*28*). Even though modified extrusion is the simplest method for producing large gel particles, many disadvantages have been linked to this procedure. Among the shortcomings displayed by this method, the main difficulty in scaling up the entire process. Also, due to the difficulties of pumping the solution through the nozzle, the required viscosity shall be lower than 200 cP.

In terms of the microgel particles, many techniques have been created to avoid the shortcomings of the simple extrusion procedure. These techniques have been categorized as modified extrusion techniques; they include:

- Jet-break-up extrusion method
- Spinning the disk
- Atomization

As for the application of the hydrogel bead encapsulation method for bioconcrete applications many investigators have implemented them obtaining different results. Fahimizadeh et al. encapsulated Bacillus pseudiformus using hydrogel beads and incorporated them into a mortar mix at 5% of the volume of the prismatic samples; then these beads were added to the middle section of the specimens (*29*). Each sample had 202 mg of capsules, which corresponds to approximately seventy-four capsules. After casting was over, the specimens were cured in distilled water for seven days. The samples were tested under three-point bending tests, for inducing cracking in the area where the capsules were located. After the cracks appeared, the samples were subjected to twelve hours of wet/dry cycles to mimic the conditions for autogenous healing through calcium carbonate precipitation. The processes occurred for 28 days when the specimens were rested under bending to determine the effect of the crack sealing on the flexural properties of the specimens. Furthermore, at 56 days of wet/dry cycles, they were also retested.

The main findings of this research include the following: the flexural strength is negatively affected by the addition of calcium alginate capsules. This situation can be mainly attributed to the water uptake capsule's ability. Past investigations have shown that the capsules are able to swell up to three times the original diameter. This capability results in favorable crack healing and the germination of spores. Furthermore, the retained water in the alginate capsules is expected to slowly be released into the cementitious matrix during the dry periods and assist in the further hydration process. Nevertheless, it occurs that the alginate capsules tend to experiment with shrinkage cracking, which can lead to defects (i.e., voids) and results in prejudicial for the integrity of the system. In terms of the flexural strength recovery after 28 days of wet/dry cycles, the specimens achieved between 15% and 30% of flexural strength recovery and up to 40% after 56 days of wet/dry cycles. Finally, the autogenous-healing products were characterized by morphological analysis, in which a field emission electron microscope was implemented. With this tool, three main calcium carbonate forms were observed, aragonite, a needle-like structure, vaterite, a calcium carbonate form that has a hexagonal unit cell shape, and calcite which corresponds to the most stable form of all. It is relevant to know that calcite has a rhombohedral unit cell structure. It is also very important to note that the author of this investigation indicated that even though different types of calcium carbonate polyphorms were observed, calcite provided the matrix with improved mechanical properties after autogenous healing, this is due because this precipitate is more stable than the others considering its higher bonding strength with cement hydrates.

Soysal et al. also researched the incorporation of hydrogel encapsulated bacteria in concrete, by using Bacillus Pseudiformus and Diaphorobacter Nitroreducens at a concentration of $10^7$ cells/ml (*12*). The two bacteria strains were encapsulated in a sodium alginate solution, that included yeast extract, along with magnesium acetate. The equipment utilized for the hydrogel bead production process was a BUCHI B-390. With the help of this equipment, the healing agent was pumped in a 450-um nozzle, then the healing agent was later turned into a laminar fluid that was separated into droplets with the help of a vibrational unit. Then, the droplets fell into a 0.1M $CaCl_2$ gelling bath subjected to an agitation rate of 200 rpm, with a magnetic stirrer, where the

droplets transformed into beads. The beads were then incorporated into a concrete mix at varying dosages depending on the cement weight. After casting, the specimens were cured for 28 days and then subjected to 28 days of wet/dry cycling, consisting of eight hours of water immersion and sixteen hours of air drying at a 50% relative humidity chamber.

For characterizing the mechanical properties of the concrete prior, the healing process, compressive strength tests, quantification of modulus of elasticity, and crack sealing efficiency monitoring were performed. The compressive strength tests 28 days after casting showed that the addition of microcapsules yielded lower results as their dosage increased. As for the modulus of elasticity, the pristine specimens did not yield a substantial difference between the different specimens. As for the crack healing efficiency analysis, the cracks were monitored with the assistance of a stereo microscope that had a digital camera attached to it, the images were taken on the cracked concrete beams while the wet/dry cycles were occurring. The image monitoring analysis was conducted on days 0,3,7,4 and 28 after cracking. As for the specimens with bacteria, the samples that displayed the best healing efficiency results were the ones with hydrogel beads at the highest concentration. The healing efficiency obtained in this investigation was approximately 57% for both bacteria strains (i.e., Diaphorobacter Nitroreducens and Bacillus pseudiformus). Nevertheless, it is relevant to note that in the overall analysis, the samples that got the best results for healing efficiency were the samples with 3% (by weight of cement) of hydrogel beads, however without any bacteria strain incorporated in them. These results reveal that the hydrogel beads can serve as a water reservoir, which can further enhance the autogenous healing in concrete

.

### *3.2.2 Vacuum Impregnation into Porous Aggregates*

Alghamri et al. (*8*) showed that it was possible to seal cracks with the impregnation of a sodium silicate solution on lightweight aggregates. For this purpose, expanded clays were impregnated with a sodium silicate solution by using a vacuum chamber pressurized at 0.7 bar (20.7 inches of mercury). The results from this investigation were encouraging, considering that the samples impregnated with this healing solution displayed a recovery in the flexural strength five times higher than the control specimens after 28 days of water curing. Furthermore, the healing of the crack depth was studied by implementing the ultrasonic pulse velocity method. Through this procedure, it was determined that the specimens that were impregnated with the sodium silicate solution presented an approximate 80 % reduction of the crack depth after 56 days of water curing compared to 21% presented by the control specimens.

Moreover, a study conducted by Wiktor and Jonkes, studied the application of this technique by vacuum impregnating a combination of bacterial spores and calcium lactate as a self-healing agent in expanded clays (*7*). The authors prepared prismatic mortar specimens incorporating the impregnated aggregates and subjected them to cracking after 56 days of curing. After being tested under bending, the beams were subjected to 100 days of water immersion, in which the crack width was monitored. From this experience, it was found that the crack width of the specimen impregnated with this healing agent could heal twice the size in comparison to the control specimens. Due to the success of these previous studies, the use of vacuum impregnation into porous aggregates was another protection technique selected.

### *3.2.3 Attachment to Cellulose Nanocrystals (CNCs)*

Cellulose is a biopolymer that is part of the plant cell wall. Cellulose fibrils show remarkable properties regarding their mechanical strength. There are two common forms of cellulose: cellulose nanocrystals (CNCs) and cellulose nanofibrils. Moreover, CNCs correspond to crystalline rod-like shape structures with a width between 3 and 5 nm and a length between 50-500 nm. Furthermore, CNCs can be extracted by different methods, including metal-catalyzed oxidation, the one that was used in this study (*30*). The addition of CNCs in concrete has shown remarkable results in terms of mechanical properties (*10*). Hence, the present report aimed at attaching the CNCs to bacteria to maximize its benefits.

In bacterial adhesion, physic-chemical properties have a vital role. According to the proximity of the microorganism to the surface, the interactions can be classified into three regions. The first one is when there is no interaction. The second one is when hydrodynamic effects take place, and the lastly the third one is electrostatic adhesion, also known as van der Walls interactions (*31*). The present report aimed at implementing electrostatic interaction as the method for attaching the bacteria to the CNCs

# 4. METHODOLOGY

## 4.1 Experimental Program for Hydrogel Beads

### *4.1.1 Healing Agent*

A suspension of 1.3% sodium alginate with the bacterial solution of *Bacillus pseudofirmus* at a concentration of $10^8$ cells/ml formed the healing agent. Three different precursors were added to the suspension. These precursors were magnesium acetate, calcium lactate, and sodium lactate at a concentration of 75mM/l. In addition, yeast extract was added at a concentration of 0.74 mM/l.

### *4.1.2 Calcium Alginate Beads Encapsulation Process*

In the literature review section, different encapsulation technologies were presented. One of the most common ones is encapsulation through hydrogel beads. This method is also known for being a secondary water source that can sustain the microbial-induced calcite precipitation (*12*). Through a procedure known as the modified extrusion process, the healing agent (i.e., 1.3% sodium alginate solution, mineral precursor, nutrient, and bacterial solution) is extruded using a BUCHI B-390 encapsulator equipment. Furthermore, Figure 1a. presents a real image of the equipment, while figure 1b represents a conceptualization of the encapsulator components. The healing agent was pressurized at 0.5 bar and went through a 450 $\mu m$ nozzle. The nozzle also counts with a vibrational unit that transforms the laminar liquid mixture into homogeneous sized droplets. Then, the droplets fell into a 0.1M calcium chloride bath (*12*), which purpose was to jellify the droplets. These jellified droplets were stirred at 200 revolutions per minute (rpm), to avoid agglomerations of the droplets falling on top of each other. Finally, the hydrogel beads were rinsed using de-ionized (DI) water and filtered with a vacuum filter, and stored in an incubator at 4°C for future use. This methodology was followed for magnesium acetate and sodium lactate precursors. However, for the calcium lactate, this one was directly added to the water of the mortar mix. Only the bacteria with the yeast extract were encapsulated into the hydrogel beads. The reason behind this situation is the fact the calcium ions of the precursor were reacting with the sodium alginate solution before reaching the encapsulator, therefore preventing the production of homogenous sized hydrogel beads.

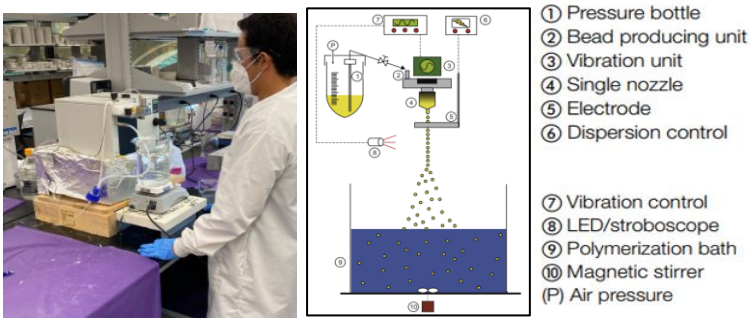


**(a)** **(b)**

**Figure 1. (a) Hydrogel Bead Encapsulation Set-Up (b) Schematics of Equipment Components**

## 4.2 Vacuum Impregnation on Porous Aggregates

### *4.2.1 Healing Agent*

A bacterial solution of *Bacillus pseudofirmus* ($10^8$ cells/ml) was used. Three precursors were added to this solution: magnesium acetate, calcium lactate, and sodium lactate at a concentration of 75 mM/l. Additionally, yeast extract was added at a concentration of 0.74 mM/L.

### *4.2.2 Vacuum Impregnation Process*

The healing agent was impregnated into expanded clays, which correspond to lightweight aggregates (LWA) using a vacuum chamber. First, the LWAs were oven-dried at 100 C and 50% relative humidity for 24 hours. After the oven drying process, the LWA was placed into the vacuum, and then the solution was added to the chamber, to be finally pressurized at 0.7 bar. It is relevant to note that to ensure proper impregnation, the solution was placed up to 20 mm above the aggregate level. Moreover, to determine the optimum submergence time, three different impregnation periods were studied: 30 minutes, 60 minutes, and 120 minutes. Figure 2 presents the respective set-up implemented for this method. After each impregnation, the specimens were taken to a centrifuge, where the samples were subjected to rotation at a speed of 200 revolutions per minute (rpm), for then being oven-dried overnight, as per TR2R1 standard (*32*). The absorption percentage was measured and calculated using equation 1. Furthermore, table 1 presents the absorption results according to the impregnation time of each precursor and bacteria combination. After analyzing the results, 60 minutes of vacuum impregnation was chosen as the optimal time, considering that no major changes in the absorption values were found.

$$Absorption\ (\%) = \frac{Mass\ of\ SSD\ specimen - Mass\ of\ oven\ dried\ specimen}{Mass\ of\ oven\ dried\ specimen} \quad (1)$$

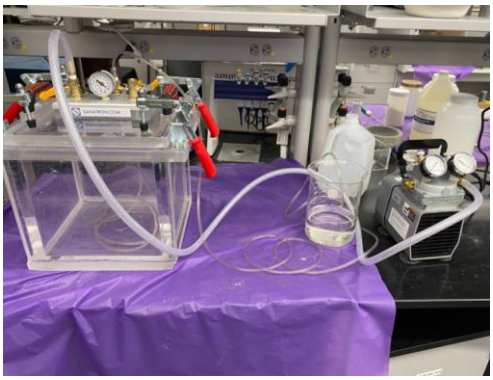

**Figure 2. Vacuum Impregnation Set-Up**

**Table 1. Absorption percentage for aggregates when submerged in different solutions**

| Self-healing solution ID | Time interval of immersion in the vacuum chamber | | |
|---|---|---|---|
| | **30 min.** | **60 min.** | **120 min.** |
| Magnesium acetate + yeast extract + bacteria | 24.4% | 24.3% | 24.45% |
| Calcium lactate + yeast extract + bacteria | 23.7% | 24.8% | 24.4% |
| Sodium lactate + yeast extract+ bacteria | 23.92% | 25.92% | 25.12% |

## 4.3 Cellulose Nanocrystals to Bacteria Attachment Process

Cellulose nanocrystals (CNC) were bought from Blue Goose Biorefineries Inc. The cationic CNCs were prepared using 25 g of 8% CNC suspension (by weight) and mixed with concentrated sodium hydroxide (NaOH) solution at 65 ℃ for 30 min. Next, 6.23 g of Epoxypropyl trimethyl ammonium chloride monomer (EPTMAC) was poured into the cationic CNC gel. The reaction took place at 65℃ for 6 h. Later, deionized (DI) water was added to the final suspension and it was put into a regenerated cellulose dialysis tube for 15 days to eliminate impurities *(26)*. Cationic CNC was characterized by measuring the zeta potential (surface charge) and also using Transmission Electron Microscope (TEM). For these analyses, the suspension was diluted to 0.02 wt.% (by weight).

Figure 3 illustrates the TEM pictures of the attachment between bacteria and CNC. It can be seen that *Bacillus pseudofirmus* bacteria is surrounded and protected by cellulose nanocrystals. The zeta potential (surface charge) was measured three times resulting in the following values for bacteria: -27.5, -26.7, and -26.7 mV (average of -26.9 mV). The surface charge for the CNC was 42.1, 39.9, and 39.5 mV (average of 40.5 mV). Since the bacteria and the CNC had opposite surface charges (negative and positive values, respectively), the interactions are mainly attributed to electrostatic forces (*33*).

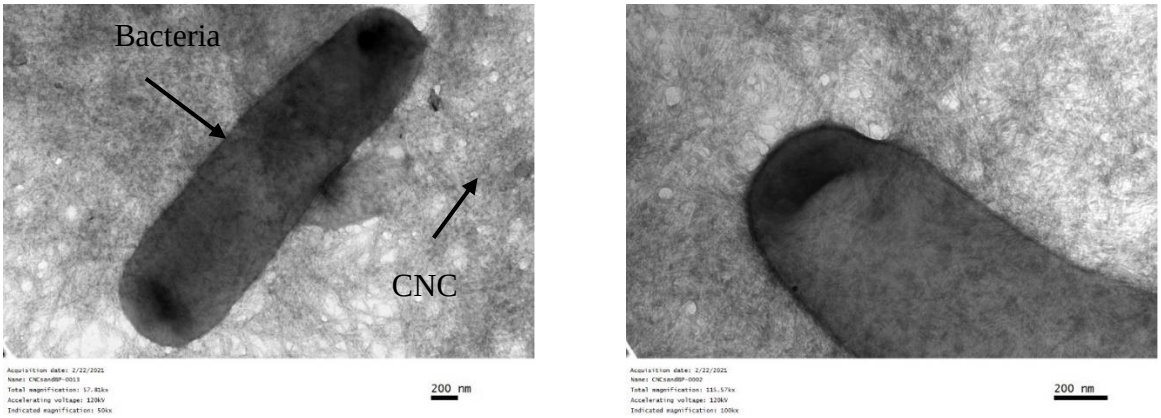


**Figure 3. TEM images of bacteria attached to the CNC**

### *4.3.1 Healing agent*

Cationic CNCs at a dosage of 0.02 % (by weight) were mixed in a volume ratio of 1:1 with the bacterial solution of *Bacillus Pseudofirmus* bacteria at a concentration of $10^8$ cells/ml. This new suspension was analyzed using Transmission Electron Microscopy (TEM) to observe their interactions as shown in Figure 3. The bacterial admixture was prepared by adding 6.22 mL/L of cationic CNC to the bacterial solution at a concentration of $10^8$ cells/ml. Three precursors were used (magnesium acetate, calcium lactate, and sodium lactate) at a concentration of 75 mM./l Additionally, yeast extract was added as a nutrient at a concentration of 1.74 mM/l

## 4.4 Experimental Matrix

Twenty-one sets of mortar specimens were prepared (three replicas of mortar cubes and three replicas of mortar beams per set). As shown in Table 2, three different precursors were implemented with and without bacteria. In addition, three sample sets without bacteria and without precursors representing each method were developed as a control (i.e., Sample 1,2,3).

**Table 2. Experimental Matrix**

| Sample ID | Description |
|---|---|
| 1 | Control no precursor, no nutrient and no bacteria |
| 2 | Control only with sand and fine lightweight aggregate |
| 3 | Control no nutrient no bacteria with CNC |
| 4 | Hydrogel with Magnesium Acetate 75 mM/l with 1.74 mM/l of yeast extract (without bacteria) |
| 5 | LWA with Magnesium Acetate 75 mM/l with 1.74 mM/l of yeast extract (without bacteria) |
| 6 | CNC with Magnesium Acetate 75 mM/l with 1.74 mM/l of yeast extract (without bacteria) |
| 7 | Hydrogel with Magnesium Acetate 75 mM/l with 1.74 mM/l of yeast extract (with bacteria) |
| 8 | LWA with Magnesium Acetate 75 mM/l with 1.74 mM/l of yeast extract (with bacteria) |
| 9 | CNC with Magnesium Acetate 75 mM/l with 1.74 mM/l of yeast extract (with bacteria) |
| 10 | Hydrogel with Calcium Lactate 75 mM/l with 1.74 mM/l of yeast extract (without bacteria) |
| 11 | LWA with Calcium Lactate 75 mM/l with 1.74 mM/l of yeast extract (without bacteria) |
| 12 | CNC with Calcium Lactate 75 mM/l with 1.74 mM/l of yeast extract (without bacteria) |
| 13 | Hydrogel with Calcium Lactate 75 mM/l with 1.74 mM/l of yeast extract (with bacteria) |
| 14 | LWA with Calcium Lactate 75 mM/l with 1.74 mM/l of yeast extract (with bacteria) |
| 15 | CNC with Calcium Lactate 75 mM/l with 1.74 mM/l of yeast extract (with bacteria) |
| 16 | Hydrogel with Sodium Lactate 75 mM/l with 1.74 mM/l of yeast extract (without bacteria) |
| 17 | LWA with Calcium Lactate 75 mM/l with 1.74 mM/l of yeast extract (with bacteria) |
| 18 | CNC with Calcium Lactate 75 mM/l with 1.74 mM/l of yeast extract (with bacteria) |
| 19 | Hydrogel with Sodium Lactate 75 mM/l with 1.74 mM/l of yeast extract (with bacteria) |
| 20 | LWA with Sodium Lactate 75 mM/l with 1.74 mM/l of yeast extract (with bacteria) |
| 21 | CNC with Sodium Lactate 75 mM/l with 1.74 mM/l of yeast extract (with bacteria) |

## 4.5 Mortar and Concrete Mix Design

Tables 3, 4, and 5 show the mortar mix design according to the encapsulation method. The mortar mix design was 1 part of cement and 2.75 parts of sand according to ASTM standard C-109 *(22)*. The water to cement ratio (w/c) and the sand to binder ratio (s/b) were 0.45 and 1.85, respectively. The nominal aggregate size for the sand was 4.65 mm. However, the impregnation of porous aggregates method implemented 50% of sand and 50% of expanded clays by weight. The nominal maximum size was 2.36 mm for the LWA aggregates. In addition, the mixture had Polyvinyl Alcohols (PVA) fibers to improve the ductility of the mortar beams, to allow failure from the bottom up to three-quarters of the height without causing sudden failure. The PVA fibers were 38 $\mu m$ in diameter and 8 mm in length and had a tensile strength of 1600 MPa, Young's modulus of 40 GPa, a maximum elongation of 5.7%, and a density of 1.3 g/cm$^3$. It is relevant to note that in the case of vacuum impregnation on LWA and for the attachment of bacteria to the CNC method the percentage of the bacterial solution to concrete volume was approximately between 15% and 18% (this value ranges depending on the precursor type and the presence of bacteria in the solution). However, in terms of the dosage of hydrogel beads, it was kept at 1.5% by the weight of cement, as per previous research work (*12*). This value represents approximately 0.84% of the bacterial solution by concrete volume. Once the best performing sample was obtained from the analysis in mortar specimens, a scale-up analysis was done in concrete samples. Table 6 presents the mixture design for concrete.

**Table 3. Mortar Mixture Proportions for Hydrogel Beads Method**

| Cement (Kg/m$^3$) | Sand (Kg/m$^3$) | Water (Kg/m$^3$) | Fibers (Kg/m$^3$) | Hydrogel Beads (Kg/m$^3$) |
|---|---|---|---|---|
| 561.8 | 1504.3 | 254.3 | 3.3 | 8.4 |

**Table 4. Mortar Mixture Proportions for Vacuum Impregnation Method**

| Cement (Kg/m$^3$) | Lightweight Aggregate (Kg/m$^3$) | Sand (Kg/m$^3$) | Water (Kg/m$^3$) | Fibers (Kg/m$^3$) |
|---|---|---|---|---|
| 475.9 | 637.6 | 637.6 | 214.1 | 6.5 |

**Table 5. Mortar Mixture Proportions for CNC Attachment Method**

| Cement (Kg/m$^3$) | Sand (Kg/m$^3$) | Water (Kg/m$^3$) | Fibers (Kg/m$^3$) | CNC+Bacteria Admixture (Kg/m$^3$) |
|---|---|---|---|---|
| 561.5 | 1506.1 | 87.2 | 6.5 | 170 |

**Table 6. Concrete Mixture Proportions**

| Cement (Kg/m$^3$) | Concrete Sand (Kg/m$^3$) | 67 Limestone (Kg/m$^3$) | Water (Kg/m$^3$) | PP Fibers (Kg/m$^3$) | Hydrogel Beads (Kg/m$^3$) |
|---|---|---|---|---|---|
| 338.17 | 785.11 | 1041.15 | 152.18 | 4.55 | 5.07 |

## 4.6 Testing

### *4.6.1 Compressive Strength Test*

After 28 days of curing, the compressive strength of the mortar cubes was measured according to ASTM C109 on the 50 mm x 50 mm samples (*34*). The specimens were tested using a hydraulic press at a constant loading rate of 124.11 MPa/min.

### *4.6.2 Flexural Strength Test*

After 28 days of curing, all the beams were tested under a three-point bending test utilizing a MARK 10 ESM 1500 equipment. For this test, the load was applied at a rate of 0.2 mm/min as prescribed by previous studies (Fahimizadeh, et al., 2020). It is relevant to note that the test was manually stopped immediately after a crack was induced in the specimen in order to avoid complete failure of the sample. The following equation was used in order to calculate the flexural strength of the specimen:

$$fs = \frac{3PL}{2\,bd^2} \quad (1)$$

where,
$fs$ = Flexural strength;
P= Peak load;
L= Span length;
b= Specimen width; and
d = Specimen height.

### *4.6.3 Self-Healing Quantification and Strength Recovery*

After the first three-point bending test, the beams of all the three protection techniques were kept under dry/wet cycles for 28 days. The cycles consisted of 16 hours of water immersion and 8 hours of drying at 38 ℃ to simulate a subtropical climate *(16)*. A stereo microscope attached with a digital camera was used to take images of the cracks at 0, 3, 7, 14 and 28 days. Then, the picture of the cracks was manually measured using the ImageJ application and an algorithm developed in Python to compute the width cracks. The flexural strength was re-measured on the 28$^{th}$ day and equation 2 was used to calculate the flexural strength recovery (FSR). Furthermore, the crack healing efficiency was calculated by implementing equation (3). Figure 4 provides a graphical

representation of the procedure implemented for determining the healing efficiency of the cracks along with flexural strength recovery.

$$\text{FSR} = (\frac{fs_f}{fs_i}) \times 100 \quad (2)$$

where,
FSR = Flexural Strength Recovery (%);
$fs_i$ = Initial flexural strength (MPa); and
$fs_f$ = Flexural Strength after 28 wet/dry cycles (MPa).

$$Healing\ Efficiency\ (\%) = \frac{W_i - W_t}{W_i} * 100 \quad (3)$$

where,
$W_i$ is the initial crack width;
$W_t$ is the crack width at a time $t$

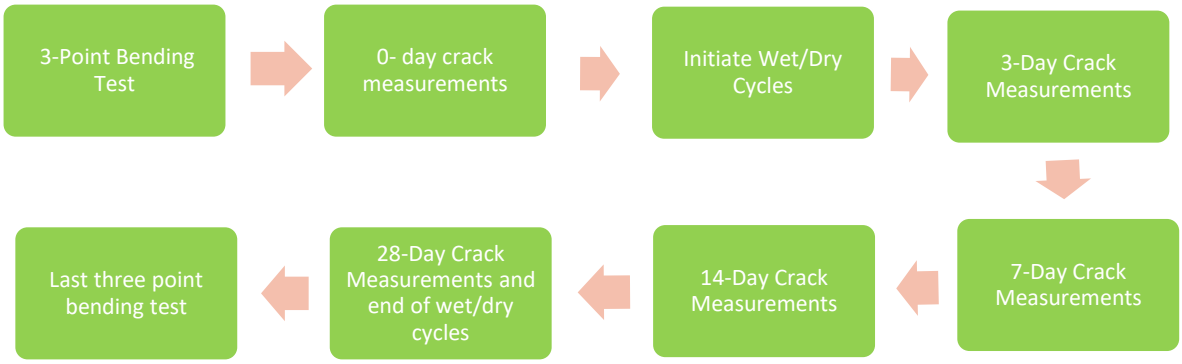


**Figure 4. Testing Sequence to Evaluate the Self-Healing on Cracked Beams.**

### *4.6.4 Characterization of Healing Products*

After the re-measuring of the flexural strength, the specimens were salvaged and cut, and a portion of the cracked face was obtained in order to platinum-coated and finally subjected to scanning electron microscopy (SEM). It is relevant to note that the specimens were not epoxy impregnated nor polished because such activities would compromise the integrity of the healing products. Lastly, the samples were subjected to x-ray energy dispersive spectroscopy (EDS) in order to determine what kind of healing products were produced by bacterial activities and further hydration of cement.

# 5. ANALYSIS AND FINDINGS

## 5.1 Compressive Strength Test Results

Figure 5 shows the average results of the compressive strength tests conducted on all the specimens sets after 28 days of curing according to the encapsulation method. A Tuckey honest significant difference (HSD) test was conducted at a significance level of 0.05 between the average values of each sample set. The results of this analysis are presented in Table 7. It is relevant to note that samples sharing at least one letter are statistically similar. Based on Figure 5, the following are observed:

- The set of specimens that showed the highest compressive strength results were samples 12,13, and 15 (the specimens containing calcium lactate as a precursor), yielding a compressive strength superior to 60 MPa). This situation is explained by the fact that calcium lactate tends to lead to the nucleation of calcite in the specimen, which acts as a filler making the cementitious matrix denser (*11*). Nevertheless, the specimen containing LWA did not reach the same results. This behavior is explained by fact that the cementitious materials with LWA have a lower density than conventional concrete due to the presence of the porous aggregate (*35*). Previous research work has shown that the porosity lowers the compressive strength of the material (*36*).
- All these specimens were statistically higher than the controls (i.e., samples 1 and 2). Nevertheless, they were not statistically different than specimen 3 (control with CNC

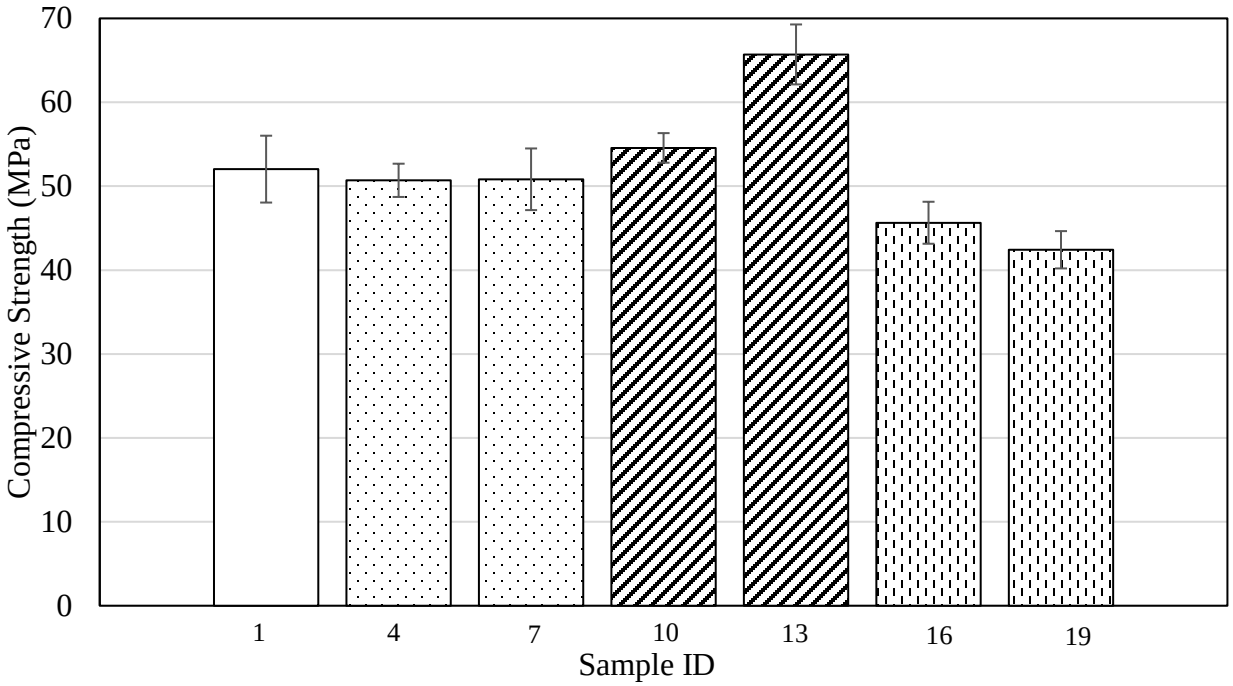


**(a)**

incorporated to the mix). This behavior is explained by the fact that the addition of CNCs to mortar specimens has shown improvements in the compressive strength (*10*).

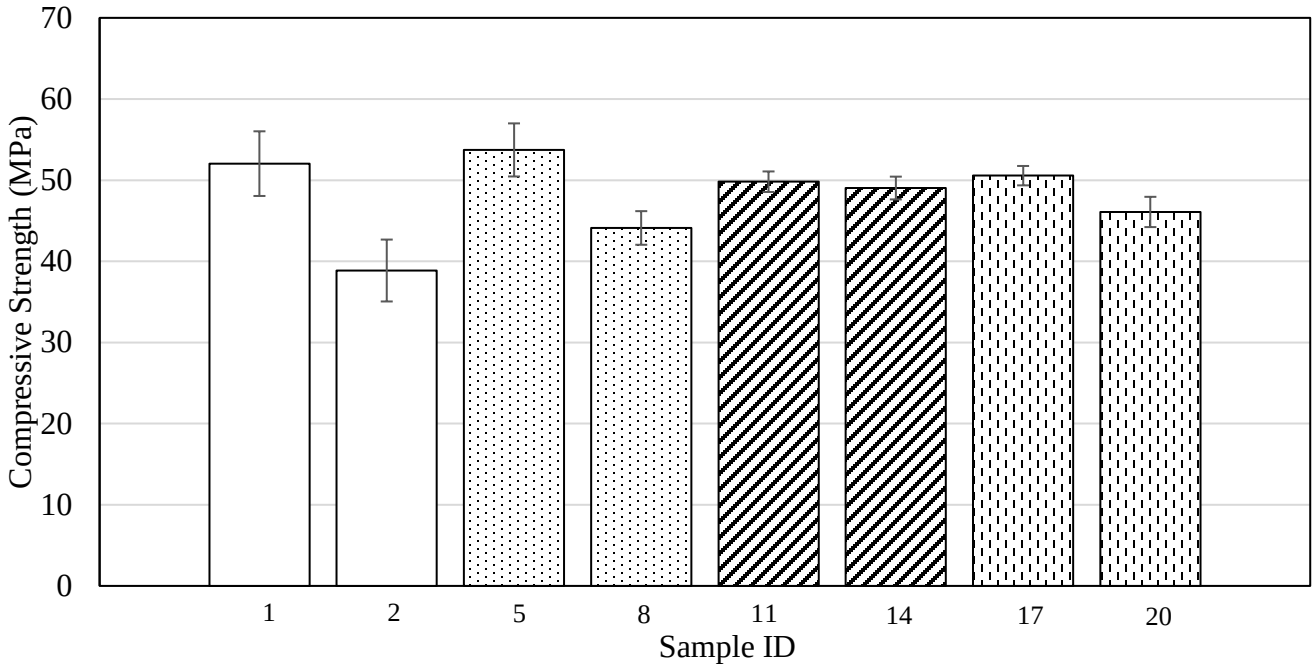


**(b)**

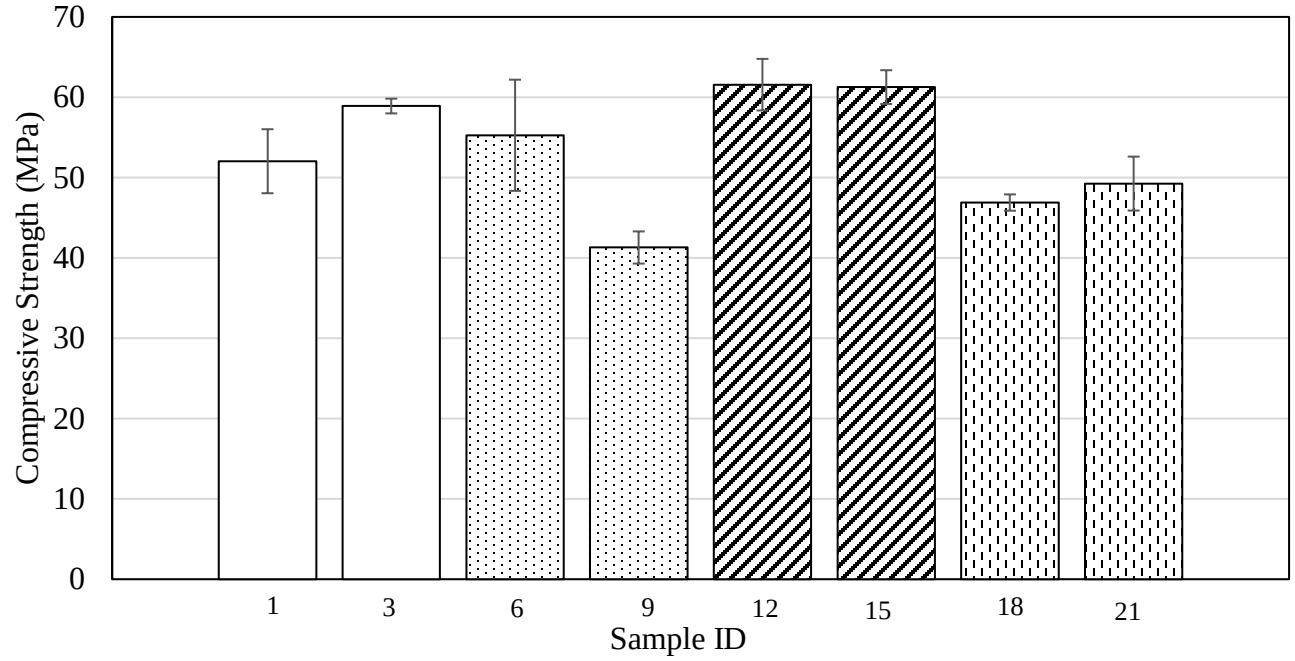


**(c)**

**Figure 5. Compressive Strength Test Results According to the Encapsulation Method (a) Hydrogel Beads (b) Vacuum Impregnation (c) CNCs Attachment**

**Table 7. Statistical Analysis for Compressive Strength Test Results**

| ID | DESCRIPTION | TUCKEY LETTER |
|---|---|---|
| 1 | Control No Nutrient No bacteria | C,D,E,F |
| 2 | Sand and fine | I |
| 3 | Sand+water+cellulose_nanocrystals | A,B,C |
| 4 | Hydro Magnesium Acetate 75mM | C,D,E,F,G |
| 5 | LWA Magnesium Acetate 75mM | C,D,E,F |
| 6 | CNC Magnesium Acetate 75mM | C,D,E,F |
| 7 | Hydro MA 75mM with Bacteria | C,D,E,F |
| 8 | LWA MA 75mM with Bacteria | F,G,H,I |
| 9 | CNC MA 75mM with Bacteria | H,I |
| 10 | Hydro Calcium Lactate 75mM | C,D,E,F,G |
| 11 | LWA Calcium Lactate 75mM | D,E,F,G,H |
| 12 | CNC Calcium Lactate 75mM | A,B |
| 13 | Hydro Calcium Lactate 75mM with Bacteria | A |
| 14 | LWA Calcium Lactate 75mM with Bacteria | C,D,E,F,G,H |
| 15 | CNC Calcium Lactate 75mM with Bacteria | A,B |
| 16 | Hydro Sodium Lactate 75mM No Bacteria | E,F,G,H,I |
| 17 | LWA Sodium Lactate 75mM No Bacteria | D,E,F,G,H |
| 18 | CNC Sodium Lactate 75mM No Bacteria | C,D,E,F,G |
| 19 | Hydro Sodium Lactate with Bacteria 75 | G,H,I |
| 20 | LWA Sodium Lactate with Bacteria 75 | E,F,G,H,I |
| 21 | CNC Sodium Lactate with Bacteria 75 | D,E,F,G,H,I |

Figure 6 displays the flexural strength results after 28 days of curing along with the flexural strength test results after 28 days of wet/dry cycles. A Tuckey HSD test was conducted at a significance level of 0.05 between the average values of each sample set. It is relevant to note that samples sharing at least one letter are statistically similar. The results of this analysis are presented in Table 8. From Figure 6, the following was observed:

- Almost all the specimens displayed similar average flexural strength after 28 days of curing. Hence, it can be concluded that no matter the encapsulation method (i.e., hydrogel beads, vacuum impregnation on LWA, and attachment to CNCs), the flexural strength of the mortar specimens will be in the range of 7 and 10 MPa.
- It is relevant to note that the remarkable results displayed in the compressive strength by the specimens containing calcium lactate as a precursor were not shown in the flexural properties. Previous work indicated that the superior properties displayed in compression by the addition of calcium lactate do not necessarily mean that the flexural strength will improve (*37*). The performance under bending is mainly dictated by the properties under tension. During bending after cracking, the neutral axis of the concrete propagates upwards, making the tensile properties rule the stress distribution of the material. In addition, the addition of calcium lactate to a concrete mix has not displayed a substantial increase in the tensile strength (*11*).
- In terms of the flexural strength after 28 days of wet/dry cycles, none of the specimens yielded a substantial difference. Furthermore, Figure 7 presents the percent flexural

strength recovery of all the specimen sets. A Tuckey HSD test at a confidence level of 0.05 was conducted to determine the statical difference in flexural strength recovery between all the samples. The results of this analysis are presented in Table 9. The vast majority of the specimens displayed a recovery that ranged between 20% and 40% of the flexural strength, which is consistent with results in previous studies (*29*).

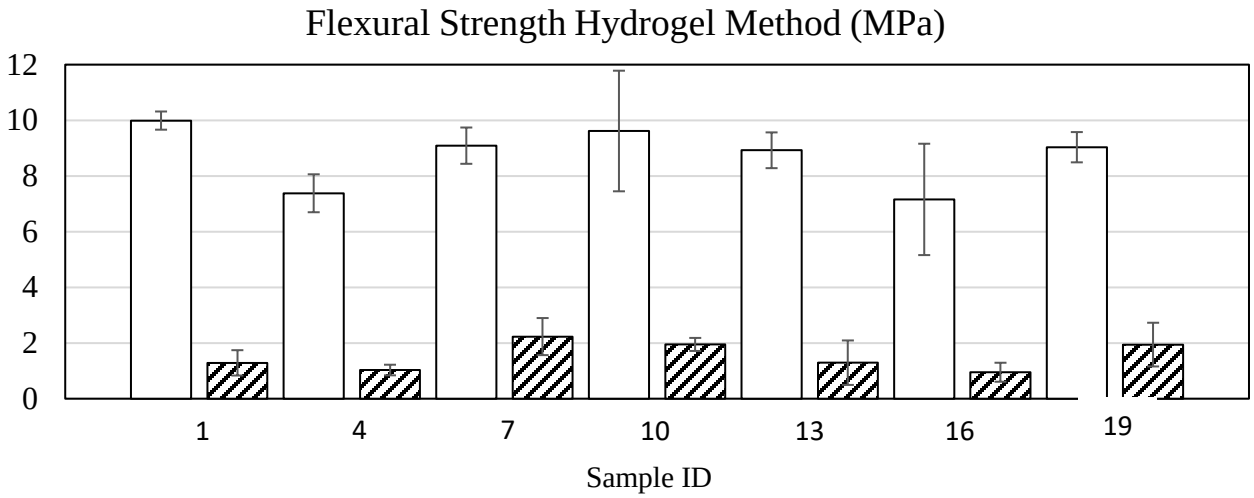


**(a)**

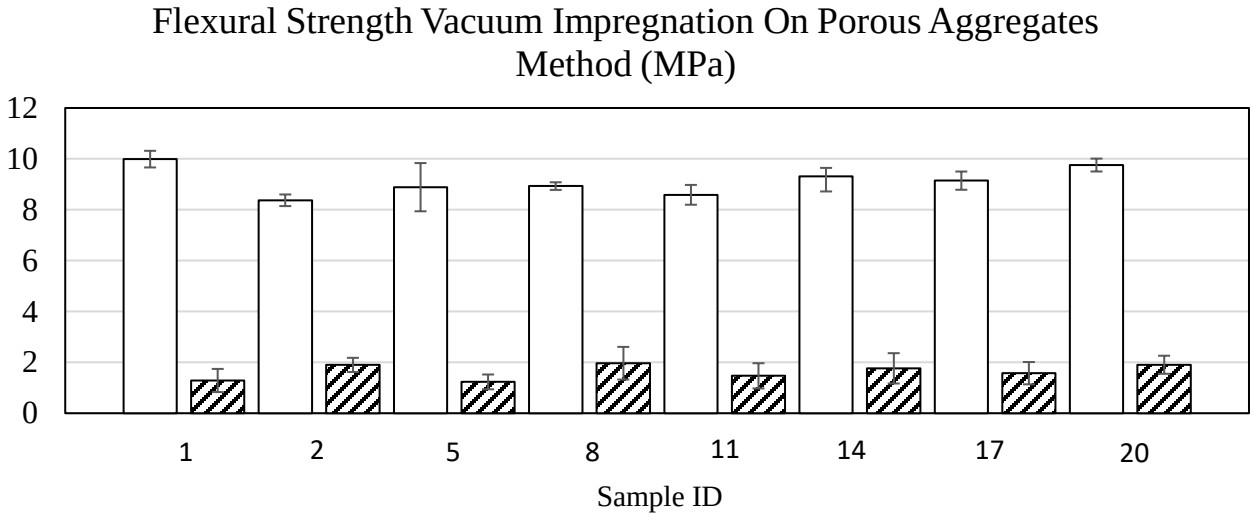


**(b)**

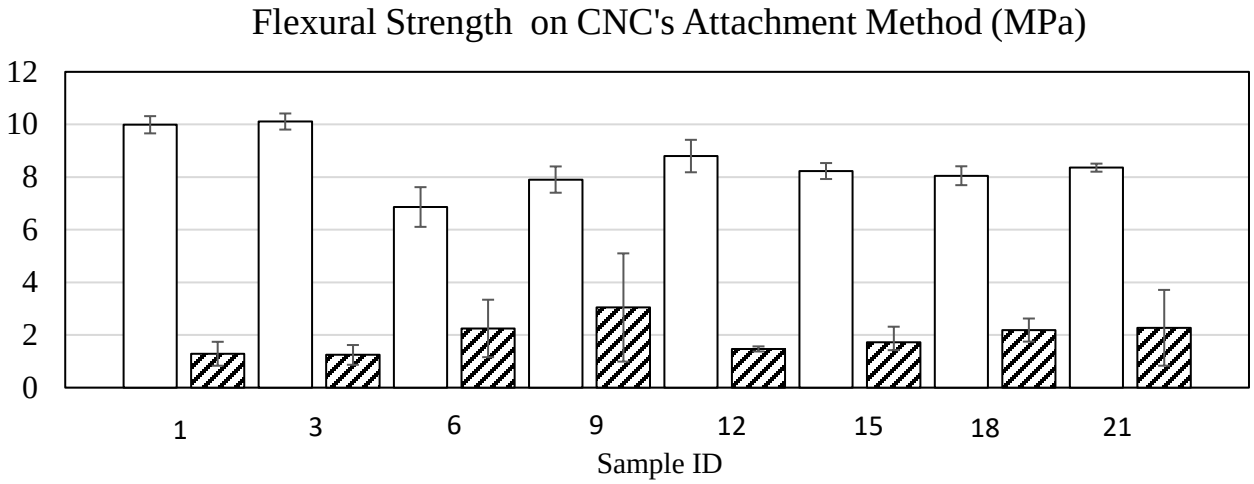


**(c)**

**Figure 6. Flexural Strength Test Results According (a) Hydrogel Beads (b) Vacuum Impregnation (c) CNCs Attachment**

**Table 8. Statistical Analysis for Flexural Strength Test Results**

| ID | DESCRIPTION | TUCKEY LETTER |
|---|---|---|
| 1 | Control No Nutrient No bacteria | A,B |
| 2 | Sand and fine | A,B,C,D |
| 3 | Sand+water+cellulose_nanocrystals | A |
| 4 | Hydro Magnesium Acetate 75mM | B,C,D |
| 5 | LWA Magnesium Acetate 75mM | A,B,C,D |
| 6 | CNC Magnesium Acetate 75mM | D |
| 7 | Hydro MA 75mM with Bacteria | A,B,C,D |
| 8 | LWA MA 75mM with Bacteria | A,B,C,D |
| 9 | CNC MA 75mM with Bacteria | A,B,C,D |
| 10 | Hydro Calcium Lactate 75mM | A,B,C |
| 11 | LWA Calcium Lactate 75mM | A,B,C,D |
| 12 | CNC Calcium Lactate 75mM | A,B,C,D |
| 13 | Hydro Calcium Lactate 75mM with Bacteria | A,B,C,D |
| 14 | LWA Calcium Lactate 75mM with Bacteria | A,B,C,D |
| 15 | CNC Calcium Lactate 75mM with Bacteria | A,B,C,D |
| 16 | Hydro Sodium Lactate 75mM No Bacteria | C,D |
| 17 | LWA Sodium Lactate 75mM No Bacteria | A,B,C,D |
| 18 | CNC Sodium Lactate 75mM No Bacteria | A,B,C,D |
| 19 | Hydro Sodium Lactate with Bacteria 75 | A,B,C,D |
| 20 | LWA Sodium Lactate with Bacteria 75 | A,B,C,D |
| 21 | CNC Sodium Lactate with Bacteria 75 | A,B,C,D |
| | All Recoveries | E |

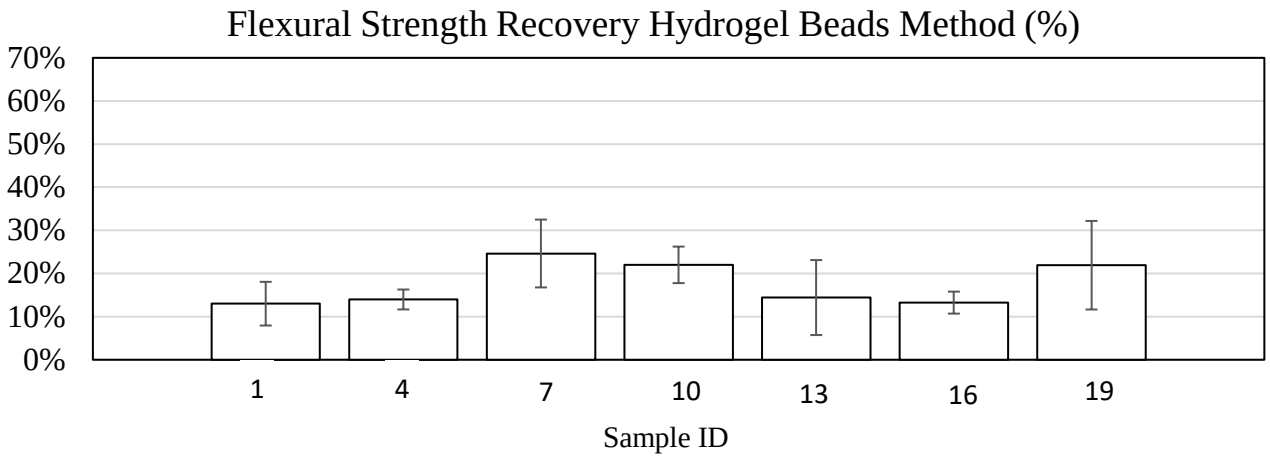


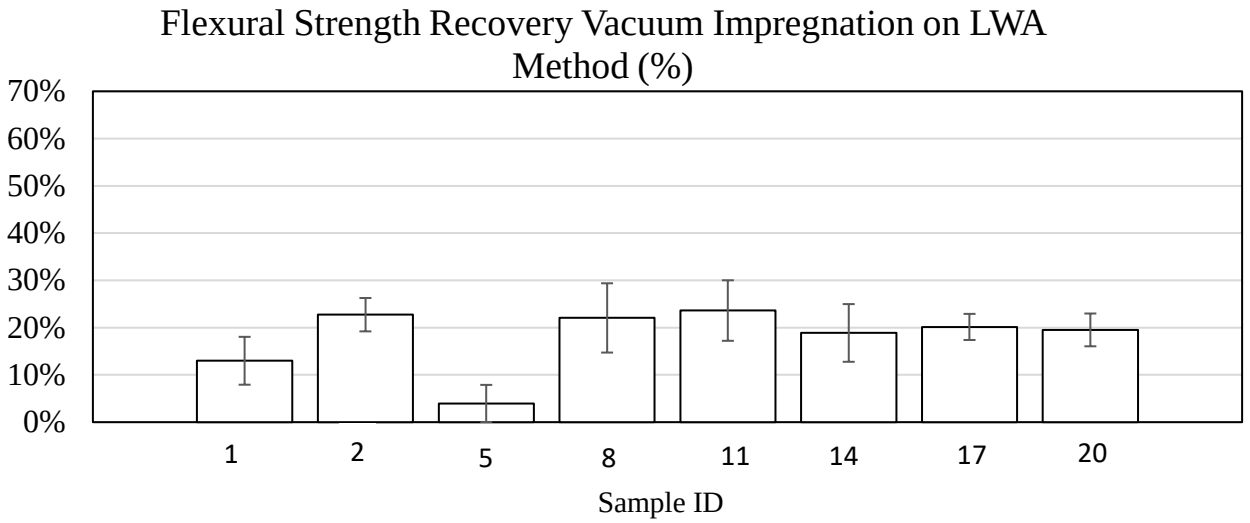


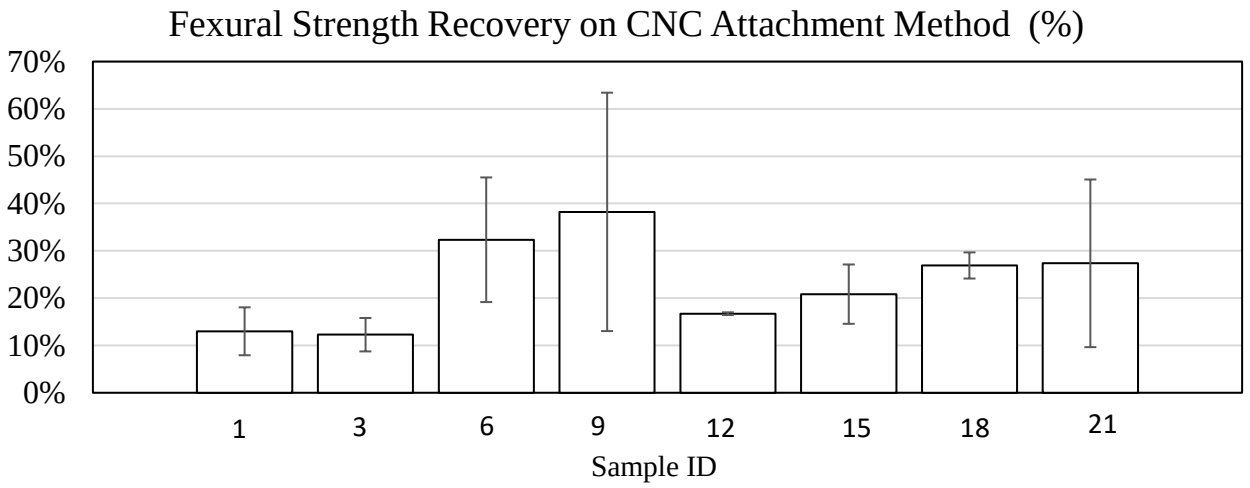


**Figure 7. Percent Flexural Strength Recovery Results According to the Encapsulation Method (a) Hydrogel Beads (b) Vacuum Impregnation (c) CNCs Attachment**

**Table 9. Statistical Analysis on Flexural Strength Recovery Results**

| ID | DESCRIPTION | TUCKEY LETTER |
|---|---|---|
| 1 | Control No Nutrient No bacteria | A |
| 2 | Sand and fine | A |
| 3 | Sand+water+cellulose_nanocrystals | A |
| 4 | Hydro Magnesium Acetate 75mM | A |
| 5 | LWA Magnesium Acetate 75mM | A |
| 6 | CNC Magnesium Acetate 75mM | A |
| 7 | Hydro MA 75mM with Bacteria | A |
| 8 | LWA MA 75mM with Bacteria | A |
| 9 | CNC MA 75mM with Bacteria | A |
| 10 | Hydro Calcium Lactate 75mM | A |
| 11 | LWA Calcium Lactate 75mM | A |
| 12 | CNC Calcium Lactate 75mM | A |
| 13 | Hydro Calcium Lactate 75mM with Bacteria | A |
| 14 | LWA Calcium Lactate 75mM with Bacteria | A |
| 15 | CNC Calcium Lactate 75mM with Bacteria | A |
| 16 | Hydro Sodium Lactate 75mM No Bacteria | A |
| 17 | LWA Sodium Lactate 75mM No Bacteria | A |
| 18 | CNC Sodium Lactate 75mM No Bacteria | A |
| 19 | Hydro Sodium Lactate with Bacteria 75 | A |
| 20 | LWA Sodium Lactate with Bacteria 75 | A |
| 21 | CNC Sodium Lactate with Bacteria 75 | A |

## 5.2 Crack Healing Efficiency

Figure 8 presents the self-healing efficiency results of cracks at the sides of the specimens at different aging stages. Based on this figure, the following observations can be drawn:

- At an early age (i.e., after 3 days of wet/dry cycles), the specimen that displayed the best results was sample 4 (the set of specimens containing magnesium acetate along with yeast extract without bacteria encapsulated in hydrogel beads). When comparing sample 4 with the rest of the specimens, no statistically significant difference was noticed.
- After 7 days of wet/dry cycles, the specimen that displayed the best results was sample 1 (the control specimen with no nutrients and no bacteria) followed by sample 11 (the set of specimens containing LWA impregnated with calcium lactate). However, no statistical difference was found.
- After 14 days of wet/dry cycles, the specimen that yielded the best results was sample 10 (the set of specimens containing calcium lactate along with yeast extract without bacteria encapsulated in hydrogel beads), followed by sample 1. However, no statistical difference was found.
- After 28 days of wet/dry cycles, the specimen that displayed the best results was still sample 10, followed by sample 1. Nevertheless, the crack healing efficiency of all the samples was statistically similar to all the samples except sample 3.

From the presented observations it can be concluded that the specimen that displayed the best results was sample 10. Even though at early stages (i.e., 3 and 7 days after wet/dry cycles) it did not show the best results, the self-healing efficiency was enhanced at later ages. Nevertheless, this sample was not statistically superior to the rest of the specimens.

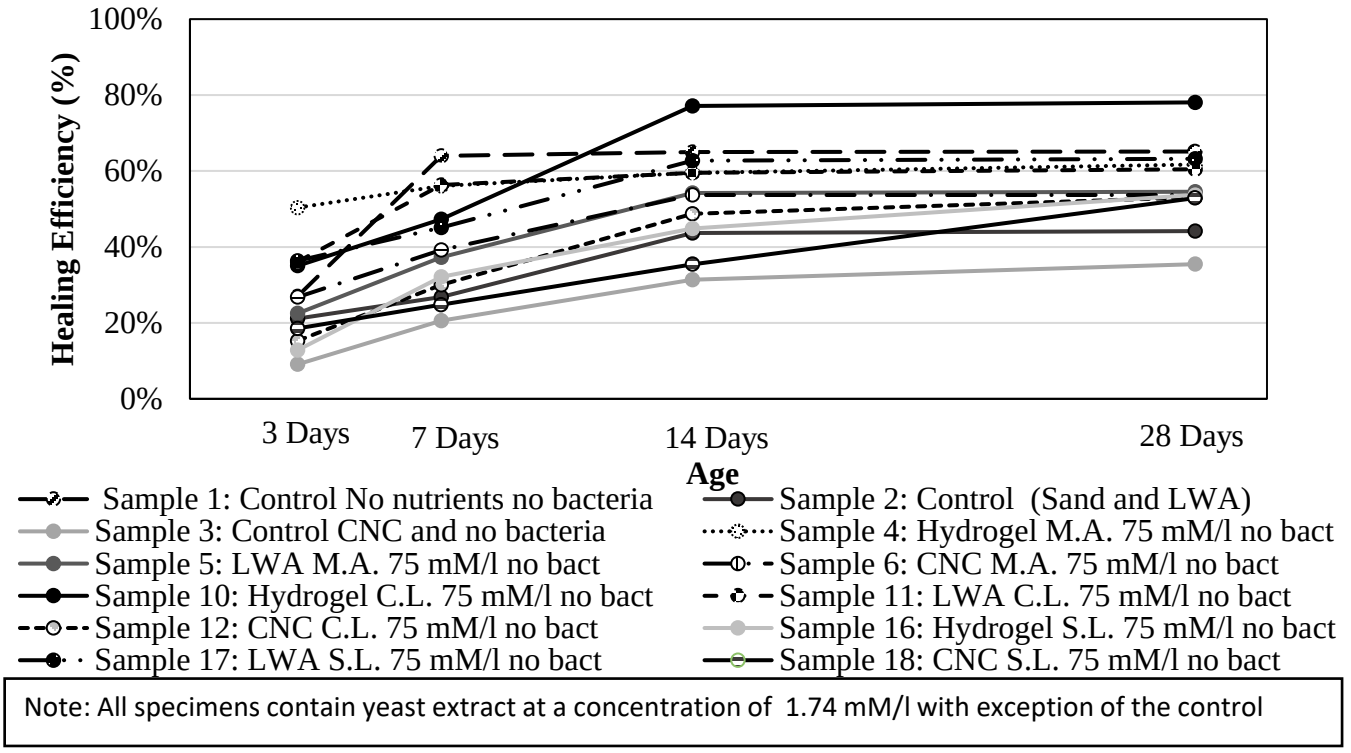


**Figure 8. Healing Efficiency at the Sides of the Specimens with Precursors without Bacteria**

In terms of the self-healing efficiency of the specimens with bacteria, Figure 9 presents the respective results. Based on Figure 9 the following observations can be made:

- At an early age of 3 days of wet/dry cycles, the specimens that displayed the best results was sample 13 (the set of specimens containing calcium lactate as a precursor along with yeast extract and bacteria encapsulated in hydrogel beads) followed by sample 15 (the set of specimens containing calcium lactate as a precursor along with yeast extract and bacteria attached to CNCs). However, no statistically significant difference was found among all the specimens; except for sample 3 (the set of specimens used as a control, in which CNCs were added).
- At 7 days of wet/dry cycles, sample 13 also provided the best results. Furthermore, this specimen was statistically similar to sample 1 (control no precursors, no nutrient, and no bacteria). At 14 days of wet/dry cycles sample 13 continued displaying the best results but kept being statistically similar to sample 1.
- Finally, at 28 days of wet/dry cycles, sample 13 also yielded the best results, followed by sample 20 (the set of specimens containing sodium lactate as a precursor along with yeast extract and bacteria impregnated in LWA). Nevertheless, they were not statistically different than the rest of the specimens, except sample 2 (set of specimens that were used as a control with 50 % of LWA as sand replacement), sample 3 (set of specimens that

were used as a control in which CNC was added) and 19 (the set of specimens containing calcium lactate as a precursor along with yeast extract and bacteria encapsulated in hydrogel beads).

Based on these observations it can be concluded that the specimen that consistently yielded the best results throughout all the wet/dry cycles process was sample 13, containing calcium lactate as a precursor along with bacteria encapsulated through hydrogel beads. Nevertheless, it was not substantially better than the rest of the specimens. It is relevant to note that even though the concentration of bacteria in the methods corresponding to vacuum impregnation on LWA and in the attachment of bacteria to CNC was significantly higher than encapsulation through hydrogel beads; they did not display the best results. A plausible reason for this situation is the fact that hydrogel beads, besides acting as a protection mechanism also act like a secondary water reservoir that can enhance the further hydration process of cement, assisting in the crack sealing(*4*). One important clarification that should be stated is that Wiktor and Jonkers obtained healing efficiency up to 100 % for an approximate initial crack width of 0.2 mm, by implementing the impregnation of porous aggregates method after 20 days of water immersion. Therefore, a final check before stating that hydrogel beads are the overall best bacterial encapsulation method shall be performed

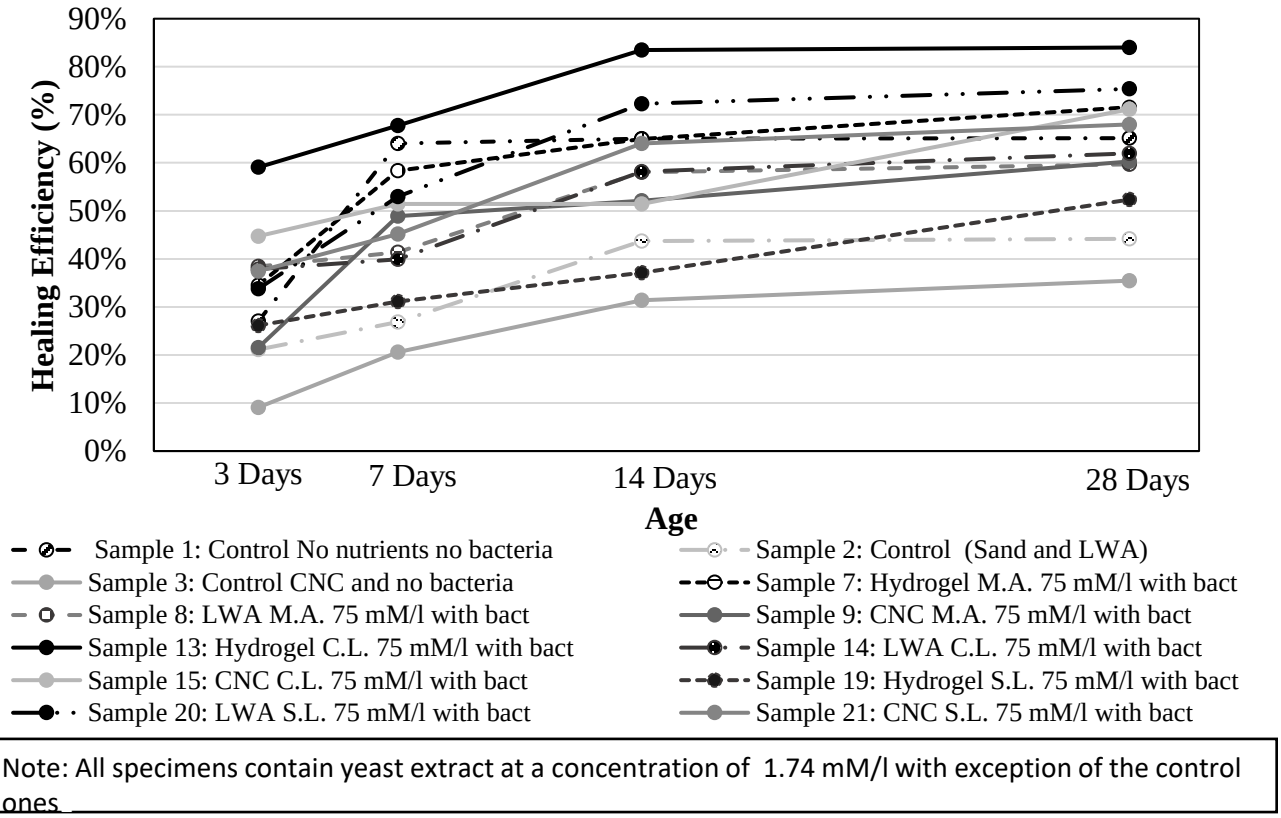


**Figure 9. Healing Efficiency at the Sides of the Specimens with Precursors and Bacteria**

## 5.3 Self-Healing Products Characterization

Figure 10 displays the secondary electron images of the spots where healing products were observed after salvaging all the samples. In addition, x-ray energy dispersive spectroscopy (EDS) was conducted on these features. Furthermore, Figures 11 and 12 present the atomic ratio plot (i.e., Aluminum/Calcium (Al/Ca) vs. Silicon/Calcium (Si/Ca)) of all the samples after processing the EDS data. According to Winter, this atomic ratio plot can indicate the presence of different types of crystals depending on their position in the plot. When the points are located at the origin, calcium-rich crystals such as ($CaCO_3$) or calcium hydroxide (CH) are plausible products. On the other hand, when the points are placed nearly between 0.45 and 0.55 on the Si/Ca axis and between 0.04 and 0.08 on the Al/Ca axis, they indicate the presence of Calcium Silicate Hydrate (CSH) like products. Furthermore, Figure 11 presents the characterization of the healing products of the specimens that did not have bacteria incorporated in the mix (i.e., only control specimens and precursors). According to the atomic ratio plot the majority of the points corresponding to the control specimens were located in the region where they are categorized as a mix of calcium-rich crystals and CSH-like products. Moreover, considering there is no presence of bacteria in these samples the plausible calcium-rich crystals are most probably CHs. In terms of the specimen that yielded the best results in terms of self-healing efficiency (i.e., sample 10) the atomic ratio plot analysis presents the points in the CSH like products region, which means that the healing product was mainly calcium silicate hydrate, meaning that the crack was sealed most probably by the further hydration cement process.

Figure 12 presents the atomic ratio plot of the specimens containing bacteria. As for this analysis, the majority of the points of the specimens that displayed the best results (i.e., sample 13, corresponding to the specimen with calcium lactate as a precursor with bacteria encapsulated in hydrogel beads) are located in the intermediate zone where the points are indicative of a combination of calcium-rich crystals or CSH like products. This behavior is explained by the fact that both bacteria and hydrogel beads act in the healing process. The deposition of calcium-rich crystals is mainly attributed to bacterial activities; while the CSH like products are mainly explained by the further hydration process of cement, which is enhanced by the combined action of the wet/dry cycles and the hydrogel beads, which act as a water reservoir (*4*). In terms of the specimen that displayed the second-best results (i.e., sample 12, corresponding to the specimen with sodium lactate as a precursor and with bacteria impregnated in the LWA), the majority of the points for this sample are also in the calcium-rich crystals plus CSH like products region. This behavior is most probably attributed to a combination of bacterial activities along with the further hydration of cement from the wet/dry cycles. It is relevant to note that the most plausible reason for the superior results obtained by the hydrogel beads encapsulation method comes from the water reservoir action, which further enhances the hydration process instead of the bacterial activities.


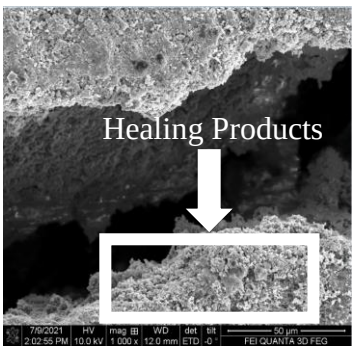


Sample 1

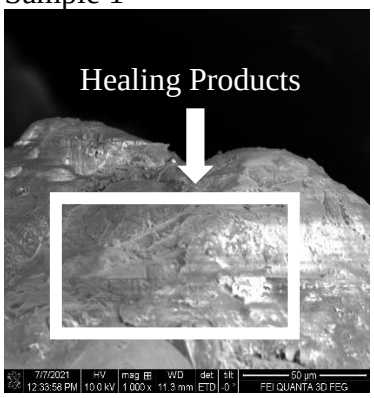


Sample 2


Sample 3


Sample 4

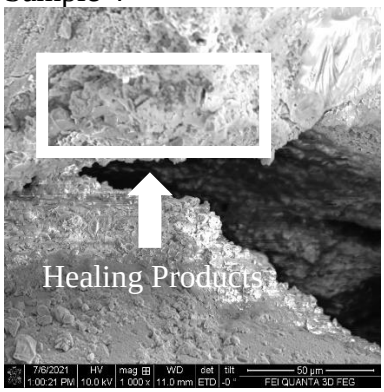


Sample 5

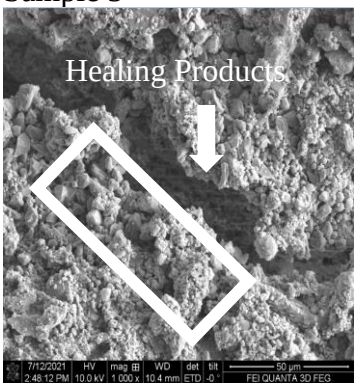


Sample 6

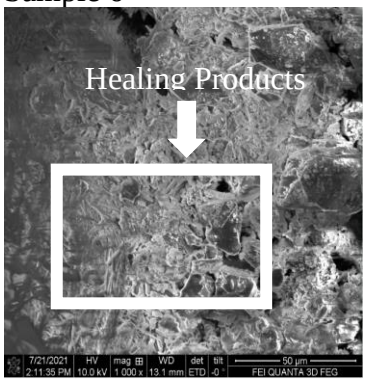


Sample 7


Sample 8


Sample 9


Sample 10

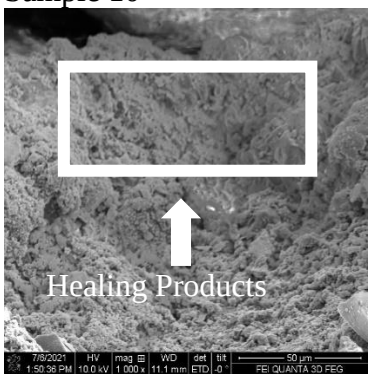


Sample 11

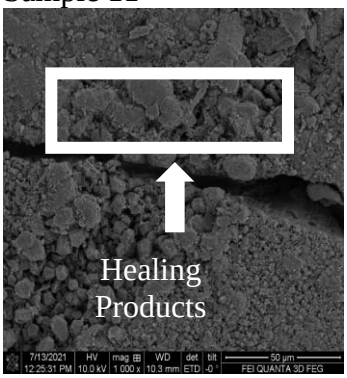


Sample 12

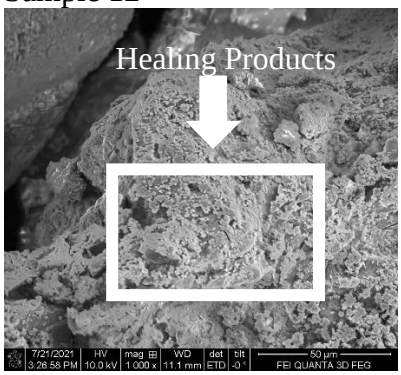


Sample 13

Sample 14

Sample 15

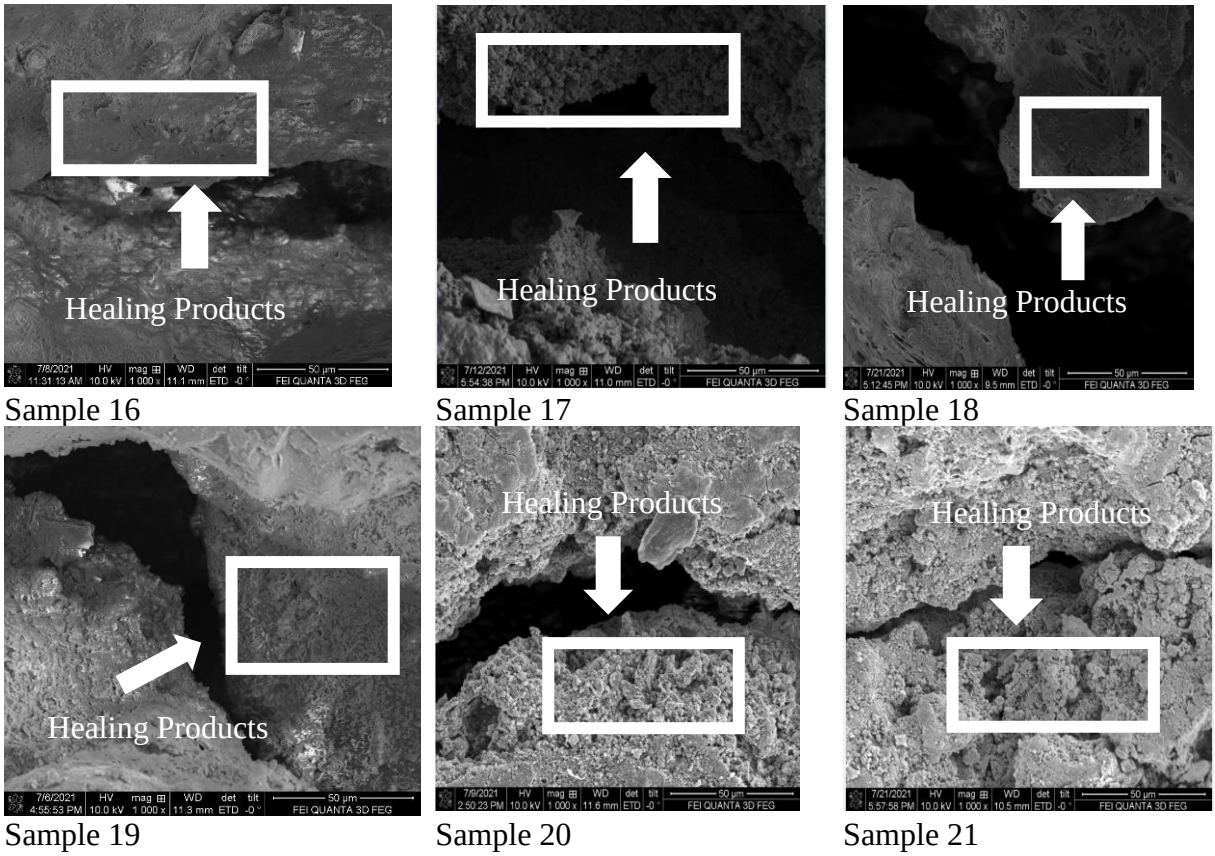


**Figure 10. Scanning Electron Images of the Healing Products**

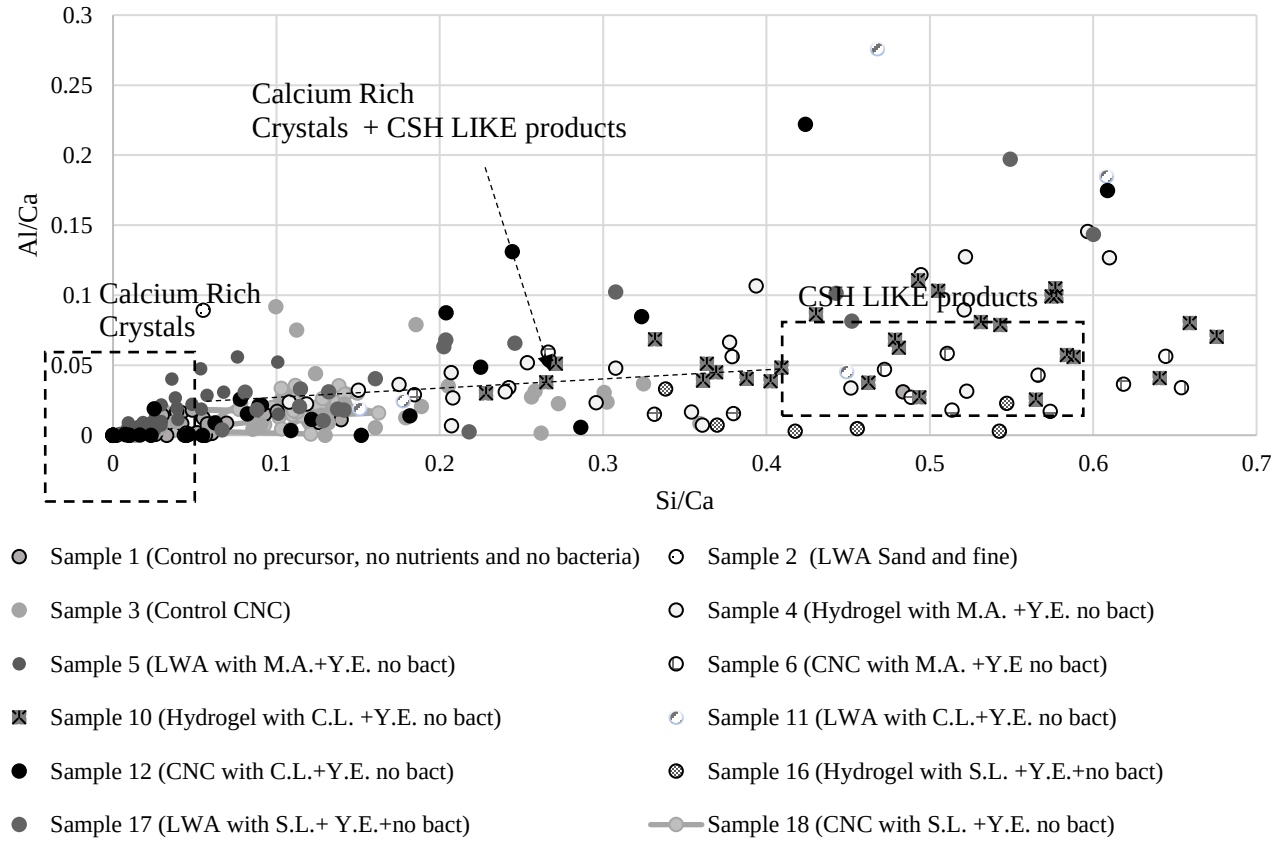


**Figure 11. Atomic Ratio Plot of Specimens only with Precursors**

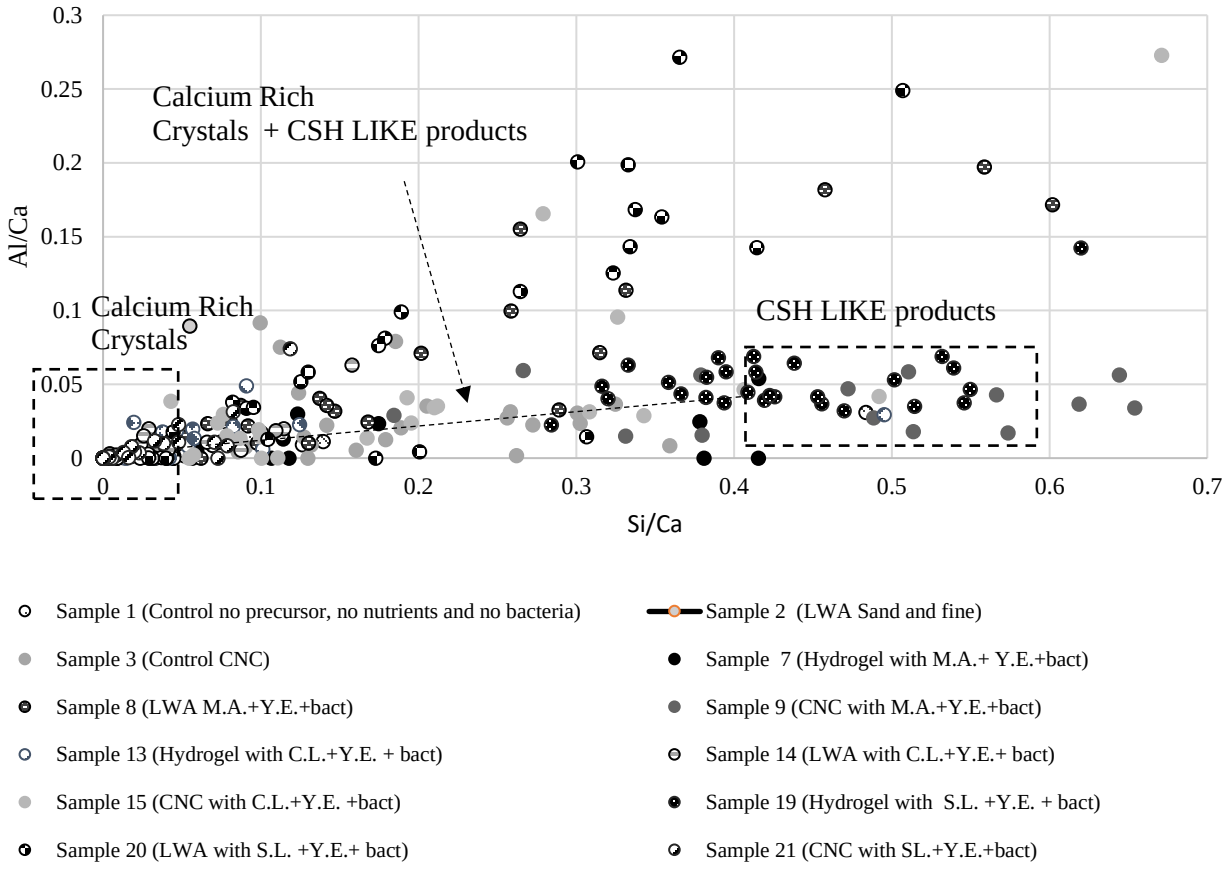


**Figure 12. Atomic Ratio Plot of Specimens with Precursors and Bacteria**

## 5.4 Concrete Compressive Strength Results

Figure 13 displays the results for the compressive strength of the concrete samples. A statistical analysis by Tuckey HSD test was performed on specimens at a confidence level of 0.05. From Figure 13, the present observations can be drawn:

- Sample B (the sample set containing calcium lactate at a concentration of 75 mM/l along with yeast extract and bacteria) showed the best results in terms of the compressive strength, which were statically significantly higher than the control specimen.
- The results from the compressive strength test were in agreement with prior studies that indicated that the incorporation of calcium lactate can route to the nucleation con calcium carbonate in the form of calcite. This aspect is beneficial for the compressive strength of the specimens since it makes the matrix denser (*11*)

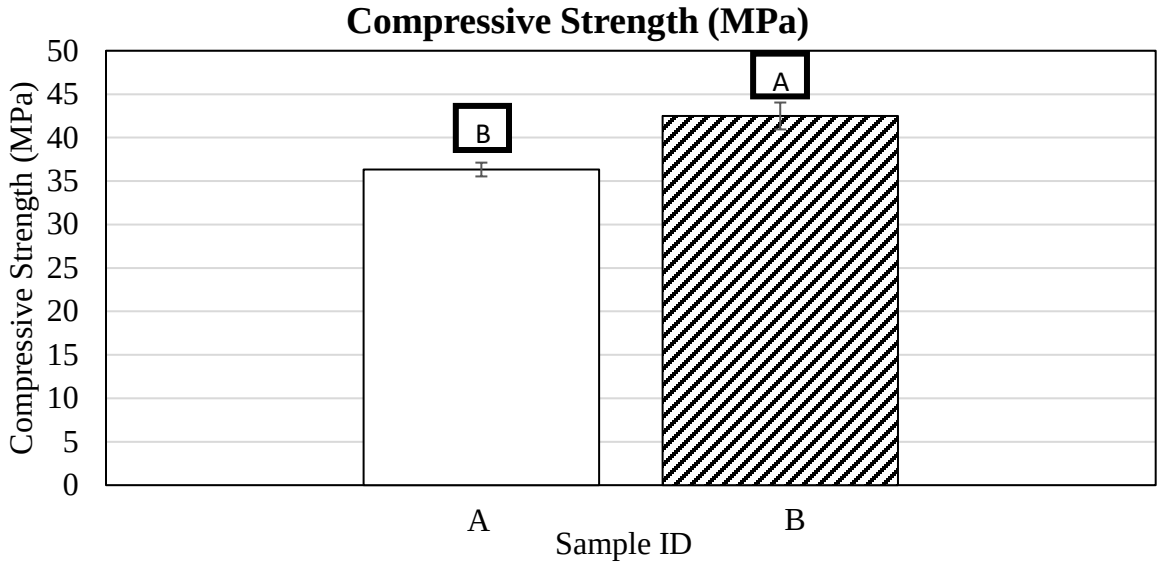


**Figure 13.Flexural Strength Results of Concrete Samples**

## 5.5 Concrete Flexural Strength and Flexural Strength Recovery Results

Figure 14 displays the flexural strength results on the concrete specimens after 28 days of curing. Furthermore, Figure 15 presents the flexural strength recovery results after the wet/dry cycling. After analyzing both figures the following observations can be drawn:

- The sample that displayed the best results was sample B (i.e., the sample containing calcium lactate at a concentration of 75 mM/l along with yeast extract and bacteria). A Tuckey HSD statistical analysis was also performed at a confidence level of 0.05, and it was found that sample B's result was statistically significantly higher than the control (Sample B).
- As for the flexural strength recovery, sample A (the control) displayed the best results. In addition, the Tuckey HSD test reveals that Sample B significantly underperformed the flexural strength recovery of sample A. The reason for his behavior is the fact that the control specimen has crack widths substantially smaller than sample B, hence the healing occurs at a faster rate

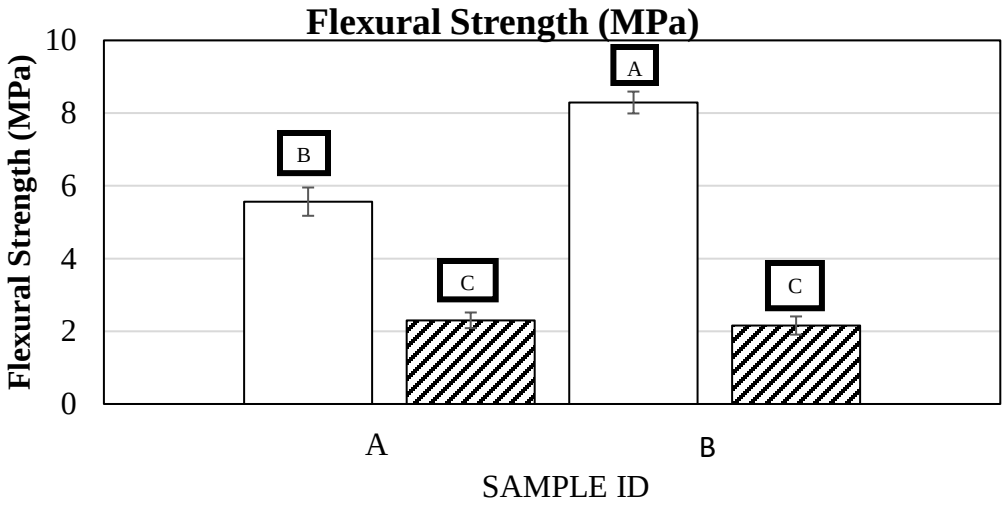


**Figure 14. Flexural Strength Results of Concrete Samples**

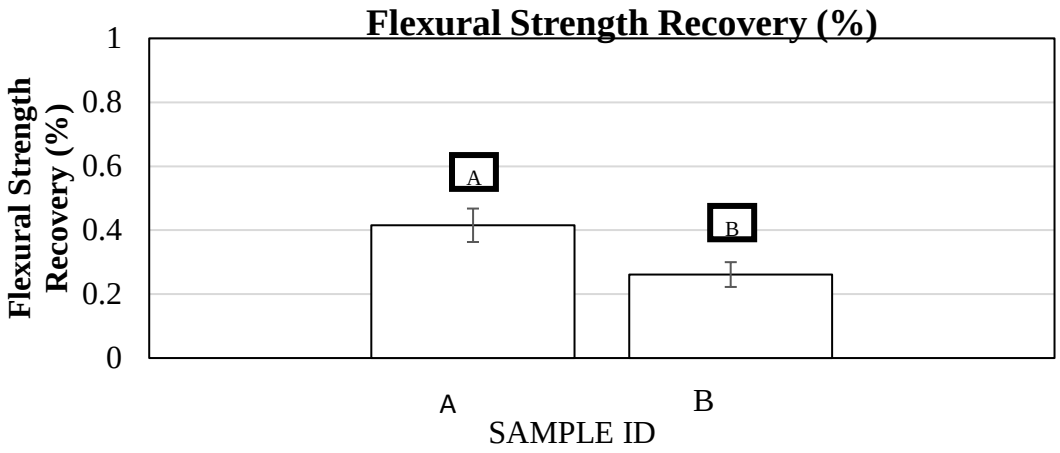


**Figure 15. Flexural Strength Recovery of Concrete Samples**

Figure 16 and Figure 17 display the healing efficiency curves of the specimens at different ages. Furthermore, the analysis was divided depending on the place of occurrence of the cracks (i.e., bottoms and sides). From the Figure 16 (analysis at the sides) the following conclusions can be drawn

- Three days after wet/dry cycles the specimen that showed the best healing efficiency was sample B (the specimen containing bacteria along with yeast extract and calcium lactate), nevertheless, the result was not statically significantly different than the control. Nevertheless, on day seven of the wet/dry cycles, the results changed, and the control specimen showed the best results
- The analyses performed on days 14 and 28 of wet/dry cycles indicated that the sample that displayed the best results was the control specimen. As a matter of fact, on day 28 of wet/dry cycles, there was a statistically significant difference between the control specimen

and Sample B. This behavior is explained by the fact that sample B had crack widths that were 1.37 times smaller than the control. Hence, the healing efficiency was lower

It is relevant to state that even though the control specimen results significantly outperformed the results from sample B; its results are encouraging. Hassan et al. also evaluated Bacillus Pseudiformus as the bacteria strain for self-healing concrete applications and turns out that the results from this investigation surpass Hassan et al. by approximately 1.58 times. However, more research at later ages (i.e., 56 and 100 days) shall be conducted to determine the long-term effect of this bacteria strain along with calcium lactate and yeast extract, since an increasing healing trend was shown

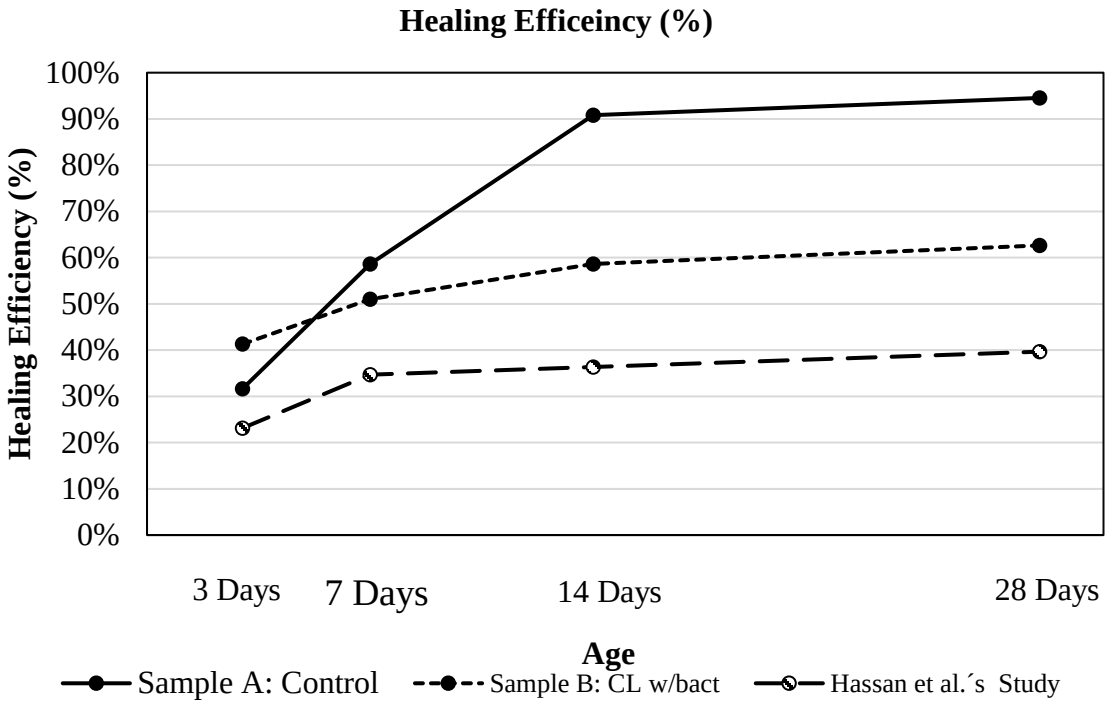


**Figure 16. Healing Efficiency of the Side Cracks of the Concrete Specimens**

Figure 17 presents the healing efficiency results of the cracks at the bottom of the specimens. From this figure the following conclusions can be drawn:

- After day 3 of wet/dry cycles, the specimen that displayed the best results was sample A (the control). Furthermore, this behavior was still noticeable on day 7 after wet/dry cycling.

- After days 14 and 28 of wet/dry cycles, the sample that display the best results was still the control. The Tuckey HSD test revealed that the difference was statistically significant. As mentioned before this behavior is mainly due to fact that the original crack width at the bottom of the control specimens is significantly smaller than sample B´s cracks. Sample B´s cracks are significantly bigger than sample A´s cracks (1.41 times).

Even considering that the control specimen displayed significantly better results compared to sample B,the results are encouraging since they outperformed Hassan et al. results for bottom cracks approximately 6.19 times. Nevertheless, this investigation needs to be extended to later ages to determine the long term effects of the healing

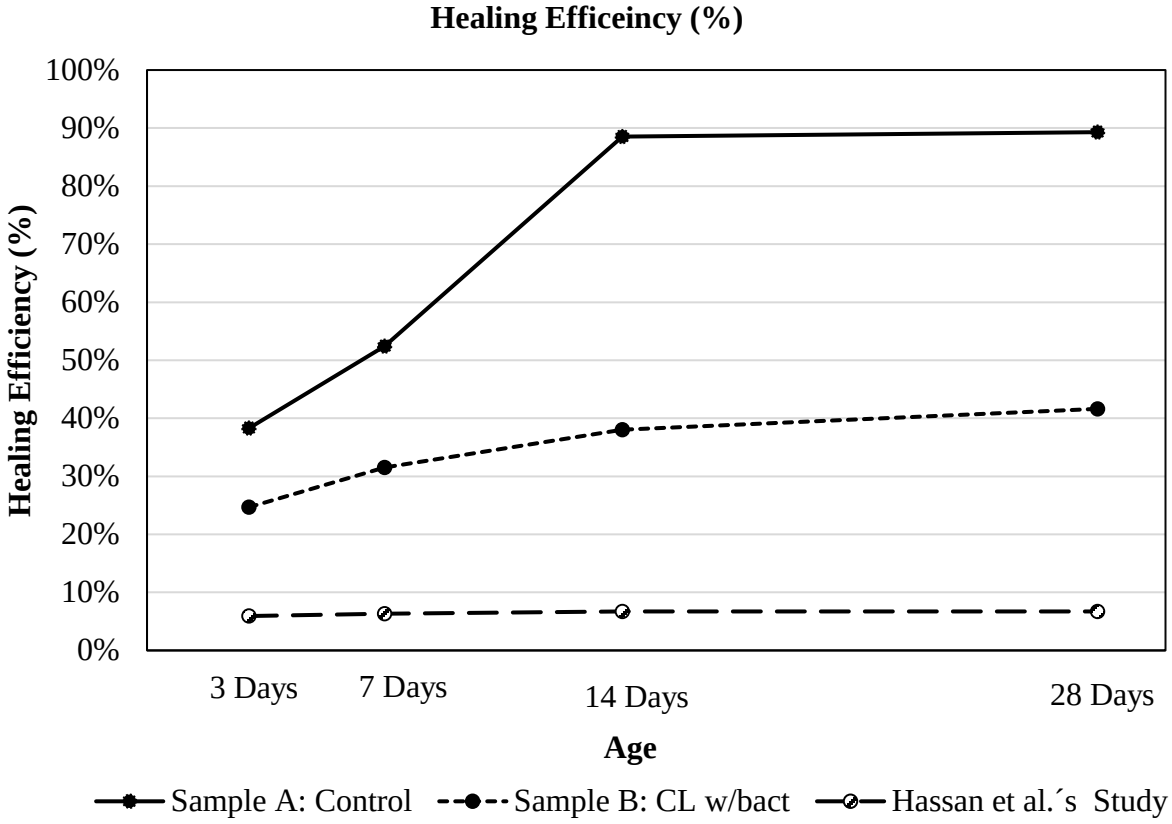


**Figure 17. Healing Efficiency Results at the Bottoms of the Cracks of the Concrete Specimens**

## 5.6 Self-Healing Product Characterizations of Concrete Specimens

Figure 18 shows the morphological analysis by backscattered electron (BSE) images of the self-healing products at a crack of the control specimen. Moreover, an energy x-ray dispersive spectroscopy (EDS) analysis was performed on this sample. From this analysis, the atomic ratio plot (presented in figure 19) was conducted. This atomic ratio plot compares Aluminum/Calcium (Al/Ca) vs. Silicon/Calcium (Si/Ca) atomic weight, and according to Winter, when the points of this plot fall into the region located at the origin, the data corresponds to calcium-rich crystals (ie., calcium hydroxide (CH) and calcium carbonate ($CaCO_3$) (*38*). The plotted points fall in this region; therefore, they are considered calcium-rich crystals; also Figure 18 shows the presence of calcite in its rhombohedral form, hence the atomic ratio plot and the BSE morphological analysis are consistent.

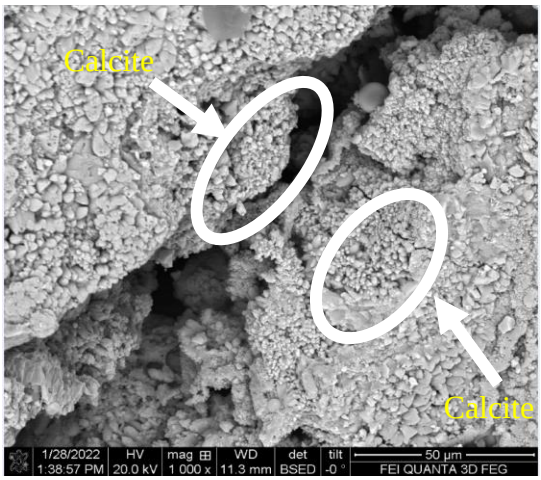


**Figure 18. SEM analysis of Concrete Control Specimen**

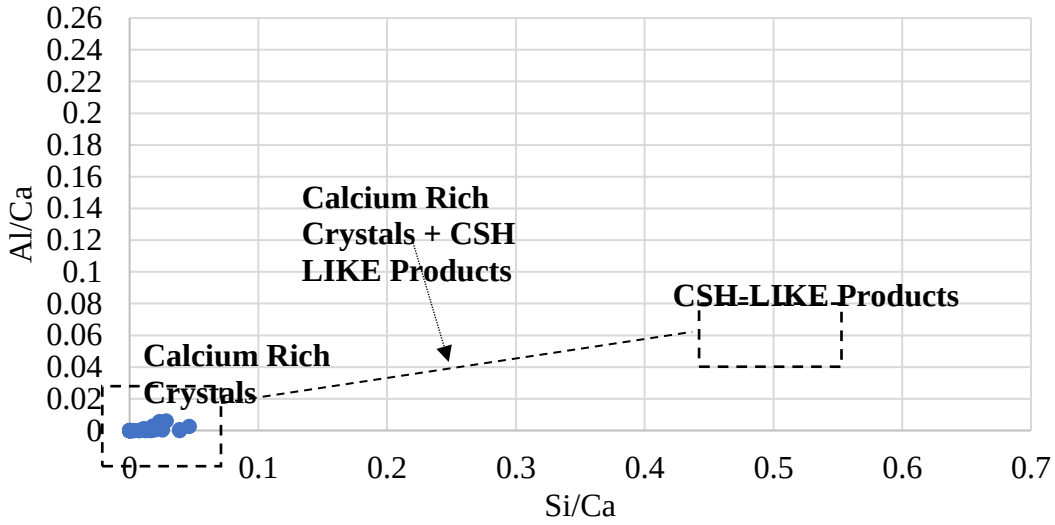


**Figure 19. Atomic ratio plot of Concrete Control Specimen**

On the other hand, Figure 20 presents the BSE images of the self-healing products at the crack of the specimen containing calcium lactate and bacteria. The morphological analysis revealed the presence of two main calcium carbonate ($CaCO_3$) forms, vaterite, and calcite. Unlike calcite vaterite has a spherical shape, also it is known that in the presence of water vaterite becomes calcite, which is an indicator that the healing products are not fully developed yet, and there is still room for more healing due to the action of the wet/dry cycles (*39*). Furthermore, EDS analysis along with the atomic ration plot (Figure 21) was also conducted at these places revealing the presence of calcium-rich crystals (since all the points fall in the origin); these results are consistent with the morphological analysis.

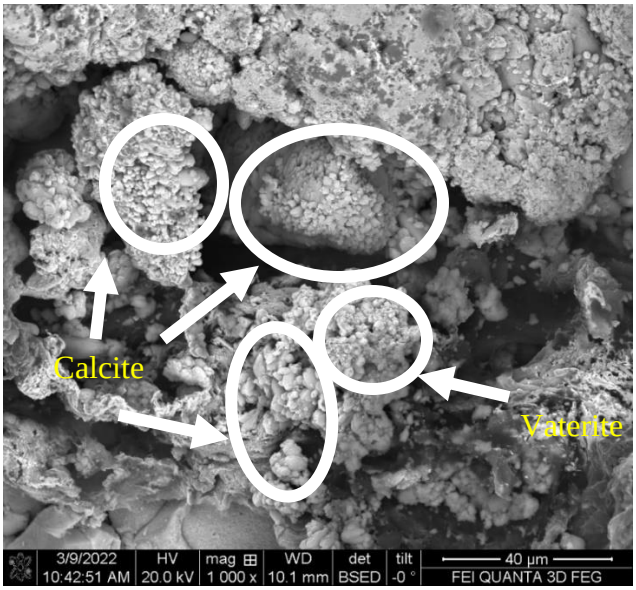


**Figure 20. SEM Analysis of the Specimen Containing Bacteria and Yeast Extract**

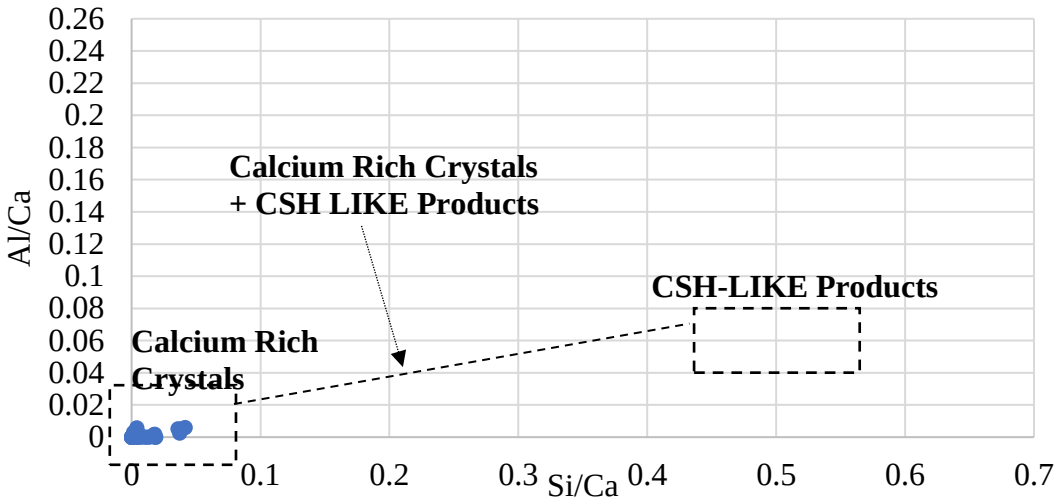


**Figure 21. Atomic Ratio Plot of Specimen Containing Bacteria and Yeast Extract**

## 6. CONCLUSIONS

The main objective of this study was to determine which parameters could optimize the crack healing efficiency of encapsulated bacteria in concrete under a subtropical climate. For this purpose, three different encapsulation methods were studied including hydrogel beads, vacuum impregnation on porous aggregates, and attachment to cellulose nanocrystals. Based on the results, the following was concluded:

- The addition of calcium lactate as a precursor has a positive effect on the compressive strength of the specimens, no matter the encapsulation method. Nevertheless, in the case of LWA specimens even though the incorporation of calcium lactate is beneficial, the porosity of the samples reduces this mechanical property.

- In terms of flexural strength, the majority of the specimens did not display a significant statistical difference. Furthermore, the flexural strength recovery of all the specimens were in the range of 20% to 40%. Moreover, no major statistically significant difference was found among all the samples.
- The cracks of the specimens were constantly monitored over a period of 28 days of wet/dry cycles. After measuring the cracks at the sides of the specimens of the cracked beams and calculating their respective self-healing efficiency, it was noticed that for the analysis of specimens only with precursors, sample 10 (the set of samples that contained calcium lactate as precursor encapsulated into hydrogel beads) displayed the best results. In terms of the self-healing efficiency for the specimens with bacteria, it was noticed that the sample that displayed the best result was sample 13, corresponding to the set of specimens containing calcium lactate as a precursor along with bacteria encapsulated in hydrogel beads. In addition, the sample that displayed the second-best results was sample 20, corresponding to the set of samples containing sodium lactate as a precursor along with bacteria impregnated into LWA. It is relevant to note that even though the specimens in which bacteria were attached to CNCs did not display the best results, sample 15 (corresponding to the specimens in calcium lactate along with CNCs attached to bacteria) displayed the most encouraging results for this particular encapsulation method.
- It is relevant to note that even though the amount of bacteria present on the hydrogel beads was inferior to the one implemented in the rest of the methods, it displayed the best results in terms of self-healing efficiency This behavior is also attributed to the reservoir action of the hydrogel beads, meaning that it was the further hydration of cement process what made the difference for the crack healing.
- The results indicated that calcium lactate corresponds to the best precursor type. Furthermore, for the encapsulation method, encapsulation in hydrogel beads showed the best results when implemented with calcium lactate as a precursor along with bacteria and yeast extract. Nevertheless, it is relevant to note that other authors have found promising results in self-healing efficiency by using calcium lactate impregnated on porous aggregates; therefore, one final check should be performed for determining the overall best encapsulation method.
- The SEM/EDS analysis conducted on the salvaged samples revealed that the specimens that yielded the best results in terms of self-healing efficiency (sample 13), had a combination of calcium-rich crystals and CSH-like products. The calcium-rich crystals are mainly considered $CaCO_3$, a product of bacterial activities. On the other hand, the CSH-like products are attributed to the hydration process of cement. This process is further enhanced by the hydrogel beads, which act as a water reservoir.

From the tests performed on concrete specimens the following conclusions were drawn:

- Adding calcium lactate is beneficial for concrete since it significantly enhanced both the compressive and flexural strength of the specimens
- The flexural strength recovery of the specimens containing calcium lactate along with yeast extract and bacteria significantly underperformed the control specimen, since wider cracks experienced lower self-healing rates
- The healing efficiency analysis was executed both at the cracks and at the sides of the specimens, indicating that the control samples had a better healing efficiency compared to the specimen containing bacteria and yeast extract. Nevertheless, these healing efficiency

results were deemed encouraging since they significantly outperformed previous works. Moreover, more investigation should be performed to determine the healing efficiency of the specimens in the long run.

- Calcite was the main self-healing product displayed by both specimens (i.e., control and samples containing calcium lactate along with yeast extract and bacteria). Nevertheless, vaterite was found in the bacteria and calcium lactate-containing specimen, which is indicative that the healing process was not finalized since vaterite becomes calcite in the presence of water. Furthermore, the EDS analysis was consistent with these findings

# 7. REFERENCES


1. Megalla, M. Bacteria Based Self - Healing Concrete Master Thesis. 2017.

2. Hassan, M. M., J. Milla, T. Rupnow, and A. Soysal. *Self-Healing Concrete Using Encapsulated Bacterial Spores in a Simulated Hot Subtropical Climate*. 2019.

3. Joshi, S., S. Goyal, A. Mukherjee, and M. S. Reddy. Microbial Healing of Cracks in Concrete : A Review. *Journal of Industrial Microbiology & Biotechnology*, Vol. 44, No. 11, 2017, pp. 1511–1525. https://doi.org/10.1007/s10295-017-1978-0.

4. Wang, J. Y., D. Snoeck, S. Van Vlierberghe, W. Verstraete, and N. De Belie. Application of Hydrogel Encapsulated Carbonate Precipitating Bacteria for Approaching a Realistic Self-Healing in Concrete. *Construction and Building Materials*, Vol. 68, 2014, pp. 110–119. https://doi.org/10.1016/j.conbuildmat.2014.06.018.

5. De Muynck, W., K. Cox, N. De Belie, and W. Verstraete. Bacterial Carbonate Precipitation as an Alternative Surface Treatment for Concrete. *Construction and Building Materials*, Vol. 22, No. 5, 2008, pp. 875–885. https://doi.org/10.1016/j.conbuildmat.2006.12.011.

6. De Belie, N. Application of Bacteria in Concrete: A Critical Evaluation of the Current Status. *RILEM Technical Letters*, Vol. 1, 2016, p. 56. https://doi.org/10.21809/rilemtechlett.2016.14.

7. Wiktor, V., and H. M. Jonkers. Quantification of Crack-Healing in Novel Bacteria-Based Self-Healing Concrete. *Cement and Concrete Composites*, Vol. 33, No. 7, 2011, pp. 763–770. https://doi.org/10.1016/j.cemconcomp.2011.03.012.

8. Alghamri R., Knellopoulos A, A.-T. A. Impregnation and Encapsulation of Lightweight Aggregates for Self Healing Concrete. 12.

9. Tziviloglou, E., V. Wiktor, H. M. Jonkers, and E. Schlangen. Bacteria-Based Self-Healing Concrete to Increase Liquid Tightness of Cracks. *Construction and Building Materials*, Vol. 122, 2016, pp. 118–125. https://doi.org/10.1016/j.conbuildmat.2016.06.080.

10. Cao, Y., P. Zavaterri, J. Youngblood, R. Moon, and J. Weiss. The Influence of Cellulose Nanocrystal Additions on the Performance of Cement Paste. *Cement and Concrete Composites*, Vol. 56, 2015, pp. 73–83. https://doi.org/10.1016/j.cemconcomp.2014.11.008.

11. Irwan, J. M., L. H. Anneza, N. Othman, A. Faisal Alshalif, M. M. Zamer, and T. Teddy. Calcium Lactate Addition in Bioconcrete: Effect on Compressive Strength and Water Penetration. *MATEC Web of Conferences*, Vol. 78, 2016, pp. 0–5. https://doi.org/10.1051/matecconf/20167801027.

12. Soysal, A., J. Milla, G. M. King, M. Hassan, and T. Rupnow. Evaluating the Self-Healing Efficiency of Hydrogel-Encapsulated Bacteria in Concrete. Vol. 2674, No. 6, 2020, pp. 113–123. https://doi.org/10.1177/0361198120917973.

13. Glatz, B. A., and K. I. Anderson. Isolation and Characterization of Mutants of Propionibacterium Strains. *Journal of Dairy Science*, Vol. 71, No. 7, 1988, pp. 1769–1776. https://doi.org/10.3168/jds.S0022-0302(88)79744-1.

14. Houtsma, P. C., M. L. Kant-Muermans, F. M. Rombouts, and M. H. Zwietering. Model for the Combined Effects of Temperature, PH, and Sodium Lactate on Growth Rates of Listeria Innocua in Broth and Bologna-Type Sausages. *Applied and Environmental Microbiology*, Vol. 62, No. 5, 1996, pp. 1616–1622. https://doi.org/10.1128/aem.62.5.1616-1622.1996.

15. Seifan, M., A. K. Samani, and A. Berenjian. Bioconcrete: Next Generation of Self-Healing Concrete. *Applied Microbiology and Biotechnology*, Vol. 100, No. 6, 2016, pp. 2591–2602. https://doi.org/10.1007/s00253-016-7316-z.

16. Dhami, N., R. S.M., and M. A. Biofilm and Microbial Applications in Biomineralized Concrete. *Advanced Topics in Biomineralization*, 2012, pp. 137–164.

17. A.M., N. Properties of Concrete. *Pearson Higher Education (4th ed.)*, 1996.

18. Erşan, Y. Ç., E. Hernandez-Sanabria, N. Boon, and N. De Belie. Enhanced Crack Closure Performance of Microbial Mortar through Nitrate Reduction. *Cement and Concrete Composites*, Vol. 70, 2016, pp. 159–170. https://doi.org/10.1016/j.cemconcomp.2016.04.001.

19. van Paassen, L. A., C. M. Daza, M. Staal, D. Y. Sorokin, W. van der Zon, and M. C. M. van Loosdrecht. Potential Soil Reinforcement by Biological Denitrification. *Ecological Engineering*, Vol. 36, No. 2, 2010, pp. 168–175. https://doi.org/10.1016/j.ecoleng.2009.03.026.

20. Karatas, I. Microbiological Improvement of the Physical. No. December, 2008.

21. Zhu, T., C. Paulo, M. L. Merroun, and M. Dittrich. Potential Application of Biomineralization by Synechococcus PCC8806 for Concrete Restoration. *Ecological Engineering*, Vol. 82, 2015, pp. 459–468. https://doi.org/10.1016/j.ecoleng.2015.05.017.

22. Erşan, Y. Ç., N. de Belie, and N. Boon. Microbially Induced CaCO3 Precipitation through Denitrification: An Optimization Study in Minimal Nutrient Environment. *Biochemical Engineering Journal*, Vol. 101, 2015, pp. 108–118. https://doi.org/10.1016/j.bej.2015.05.006.

23. Jonkers, H. M., A. Thijssen, G. Muyzer, O. Copuroglu, and E. Schlangen. Application of Bacteria as Self-Healing Agent for the Development of Sustainable Concrete. *Ecological Engineering*, Vol. 36, No. 2, 2010, pp. 230–235. https://doi.org/10.1016/j.ecoleng.2008.12.036.

24. Wang, J. Y., H. Soens, W. Verstraete, and N. De Belie. Self-Healing Concrete by Use of Microencapsulated Bacterial Spores. *Cement and Concrete Research*, Vol. 56, 2014, pp. 139–152. https://doi.org/10.1016/j.cemconres.2013.11.009.

25. Ching, S. H., N. Bansal, and B. Bhandari. Alginate Gel Particles–A Review of Production Techniques and Physical Properties. *Critical Reviews in Food Science and Nutrition*, Vol. 57, No. 6, 2017, pp. 1133–1152. https://doi.org/10.1080/10408398.2014.965773.

26. Blandino, A., M. Macías, and D. Cantero. Formation of Calcium Alginate Gel Capsules: Influence of Sodium Alginate and CaCl2 Concentration on Gelation Kinetics. *Journal of Bioscience and Bioengineering*, Vol. 88, No. 6, 1999, pp. 686–689. https://doi.org/10.1016/S1389-1723(00)87103-0.

27. Thu, B., P. Bruheim, T. Espevik, O. Smidsrød, P. Soon-Shiong, and G. Skjåk-Bræk. Alginate Polycation Microcapsules: II. Some Functional Properties. *Biomaterials*, Vol. 17, No. 11, 1996, pp. 1069–1079. https://doi.org/10.1016/0142-9612(96)85907-2.

28. Ouwerx, C., N. Velings, M. M. Mestdagh, and M. A. V. Axelos. Physico-Chemical Properties and Rheology of Alginate Gel Beads Formed with Various Divalent Cations. *Polymer Gels and Networks*, Vol. 6, No. 5, 1998, pp. 393–408. https://doi.org/10.1016/S0966-7822(98)00035-5.

29. Fahimizadeh, M., A. D. Abeyratne, L. S. Mae, R. K. R. Singh, and P. Pasbakhsh. Biological Self-Healing of Cement Paste and Mortar by Non-Ureolytic Bacteria Encapsulated in Alginate Hydrogel Capsules. 2020.

30. Reid, M. S., M. Villalobos, and E. D. Cranston. Benchmarking Cellulose Nanocrystals: From the Laboratory to Industrial Production. *Langmuir*, Vol. 33, No. 7, 2017, pp. 1583–1598. https://doi.org/10.1021/acs.langmuir.6b03765.

31. Hori, K., and S. Matsumoto. Bacterial Adhesion: From Mechanism to Control. *Biochemical Engineering Journal*. 3. Volume 48, 424–434.

32. LA DOTD, L. TR2R1: Method for Determing the Relative Density, Specific Gravity, Moisture Content and Absorption of Lightweight Aggregate. 2019, pp. 2–7.

33. Israelachvili, J. N. Intermolecular and Surface Forces. *Intermolecular and Surface Forces*. iii.

34. C109/109M-16a, A. Standard Test Method for Compressive Strength of Hydraulic Cement Mortars (Using 2-in. or Cube Specimens). *Annual Book of ASTM Standards*, Vol. 04, 2016, pp. 1–10. https://doi.org/10.1520/C0109.

35. Dilli, M. E., H. N. Atahan, and C. Şengül. A Comparison of Strength and Elastic Properties between Conventional and Lightweight Structural Concretes Designed with Expanded Clay Aggregates. *Construction and Building Materials*, Vol. 101, 2015, pp. 260–267. https://doi.org/10.1016/j.conbuildmat.2015.10.080.

36. Chen, X., S. Wu, and J. Zhou. Influence of Porosity on Compressive and Tensile Strength of Cement Mortar. *Construction and Building Materials*, Vol. 40, No. August 2016, 2013, pp. 869–874. https://doi.org/10.1016/j.conbuildmat.2012.11.072.

37. Reddy, P. N., and B. V. Kavyateja. Experimental Study on Strength Parameters of Self Repairing Concrete. *Annales de Chimie: Science des Materiaux*, Vol. 43, No. 5, 2019, pp. 305–310. https://doi.org/10.18280/acsm.430505.

38. Winter, N. B. Scanning Electron Microscopy of Cement and Concrete.

39. Omari, A., I.S. Rashid, N. A. Qinna, A. M. Jaber, and A. A. Badwan. Calcium Carbonate. 2016.